Calcium Signals Recorded from Cut Frog Twitch Fibers Containing Antipyrylazo III

JAMES MAYLIE, MALCOLM IRVING, NING LEUNG SIZTO, and W. KNOX CHANDLER

From the Department of Physiology, Yale University School of Medicine, New Haven, Connecticut 06510

ABSTRACT The Ca indicator antipyrylazo III was introduced into cut frog twitch fibers by diffusion (Maylie, J., M. Irving, N. L. Sizto, and W. K. Chandler. 1987. *Journal of General Physiology*. 89:41–81). Like arsenazo III, antipyrylazo III was largely bound to or sequestered by intracellular constituents; on average, a fraction 0.68 was so immobilized. After action potential stimulation, there was an early change in absorbance, with a wavelength dependence that nearly matched a cuvette Ca-difference spectrum. As with arsenazo III, this signal became prolonged as experiments progressed. In a freshly prepared cut fiber containing 0.3 mM indicator, the absorbance change had an average half-width of 10 ms at 18°C. The peak amplitude of this Ca signal depended on the indicator concentration in a roughly parabolic manner, which is consistent with a 1:2 stoichiometry for Ca:indicator complexation and, for indicator concentrations ≤0.4 mM, constant peak free [Ca]. If all the antipyrylazo III inside a fiber can react normally with Ca, peak free [Ca] is 3 μM at 18°C. If only freely diffusible indicator can react, the estimate is 42 μM. The true amplitude probably lies somewhere in between. The time course of Ca binding to intracellular buffers and of Ca release from the sarcoplasmic reticulum is estimated from the 3- and 42-μM myoplasmic [Ca] transients. After action potential stimulation, the release waveform is rapid and brief; its latency after the surface action potential is 2–3 ms and its half-width is 2–4 ms. This requires rapid coupling between the action potential in the transverse tubular system and Ca release from the sarcoplasmic reticulum. The peak fractional occupancy calculated for Ca-regulatory sites on troponin is 0.46 for the 3-μM transient and 0.93 for the 42-μM transient. During a 100-ms tetanus at 100 Hz, the corresponding fractional occupancies are 0.56 and 0.94. The low value of occupancy associated with the low-amplitude [Ca] calibration seems inconsistent with a brief tetanus being able to produce near-maximal activation (Blinks, J. R., R. Rudel, and S. R. Taylor. 1978. *Journal of Physiology*. 277:291–323; Lopez, J. R., L. A. Wanck, and S. R. Taylor. 1981. *Science*. 214:79–82).

Address reprint requests to Dr. W. Knox Chandler, Department of Physiology, 333 Cedar Street, New Haven, CT 06510. Dr. Irving's present address is Department of Biophysics, King's College London, 26-29 Drury Lane, London WC2B 5RL, England. Dr. Sizto's present address is 3154 Waugh Place, Fremont, CA 94536.

J. GEN. PHYSIOL. © The Rockefeller University Press · 0022-1295/87/01/0083/61 $1.00

Volume 89 January 1987 83–143

INTRODUCTION

The experiments described in this article were undertaken to study Ca transients in cut muscle fibers with antipyrylazo III. This Ca indicator, introduced to physiologists by Scarpa et al. (1978), was first used in skeletal muscle by Kovacs et al. (1979). It reacts rapidly with Ca (Scarpa et al., 1978) to form 1:1, 1:2, and 2:2 Ca:indicator complexes (Palade and Vergara, 1981). With the concentrations normally encountered in muscle experiments, 0.1–1 mM antipyrylazo III and <0.1 mM free [Ca], the predominant stoichiometry is 1 Ca:2 indicator molecules (Rios and Schneider, 1981). Although antipyrylazo III does not complex Ca with a simple 1:1 stoichiometry or select perfectly against Mg and protons, it is free from some of the problems associated with arsenazo III, such as the presence of at least two different complexes that form at different rates (Baylor et al., 1983*b*; Quinta-Ferreira et al., 1984*a*). When our experiments were started, antipyrylazo III was thought to be the best metallochromic indicator available for measuring myoplasmic Ca transients.

Once the experiments got underway, however, we found that, inside a fiber, most of the antipyrylazo III, like arsenazo III (Maylie et al., 1987*b*), was bound to or sequestered by myoplasmic constituents. This article describes some of the characteristics of this binding or sequestration. It also describes antipyrylazo III Ca signals produced by either action potential stimulation or voltage-clamp depolarization. Apart from a possible 1–2-ms delay (Baylor et al., 1985), these signals probably monitor the time course of the myoplasmic free [Ca] transient rather accurately. Since it is not known whether immobilized indicator molecules can react normally with Ca, however, the magnitude of the transient, based on cuvette calibrations, is uncertain. Two extreme calibrations, which should bracket the actual myoplasmic one, have been used to estimate free [Ca]: the low calibration assumes that all the indicator is available to react normally with Ca, whereas the high one assumes that only freely diffusible indicator can react. The low Ca calibration predicts only half-saturation of the Ca-regulatory sites on troponin during a brief tetanus; this seems insufficient to account for nearly maximum activation being achieved under this condition (Blinks et al., 1978; Lopez et al., 1981). The high Ca calibration, on the other hand, does predict almost maximum saturation of the Ca-regulatory sites. Many of the physiologically interesting conclusions from the experiments hold for either calibration.

A preliminary report of some of this work has been given (Irving et al., 1985).

METHODS

The experimental methods and analysis are described in the preceding two articles (Irving et al., 1987; Maylie et al., 1987*b*). Cut muscle fibers were mounted in a double-Vaseline-gap chamber and the membrane potential in the central region was held at −90 mV. The Ca indicator antipyrylazo III (ICN K&K Laboratories, Inc., Plainview, NY) was introduced by diffusion from the end pools, where the membranes had been made permeable by saponin treatment or, in one experiment, notches. The total concentration of indicator at the site of optical recording in the central region, denoted by $[Ap]_T$, was estimated from the absorbance at 550 nm; this was measured with a 10-nm bandpass filter and corrected for the intrinsic contribution from the fiber. Antipyrylazo III absorbance at

550 nm is insensitive to pH (near neutrality) and millimolar amounts of free [Mg]. It is sensitive to Ca but the resting level is too low to have any appreciable effect. Beer's law (Eq. 3 in Maylie et al., 1987*b*) was used to calculate, from $A(550)$, the concentration of antipyrylazo III in the myoplasmic water; the molar extinction coefficient, $\epsilon(550)$, was taken to be 2.55×10^4 M^{-1} cm^{-1} (Rios and Schneider, 1981), and the optical path length, l, was taken to be 0.7 times fiber diameter (Baylor et al., 1983*a*). The value of $\epsilon(550)$ was considered constant, although Baylor et al. (1986) have found a small concentration dependence in cuvette calibrations, which they attribute to dimer formation.

The antipyrylazo III–related absorbance change, $\Delta A(720)$, was used with Beer's law to estimate changes in the concentration of the Ca:indicator complex, $[CaAp_2]$; the stoichiometry of Ca:indicator was assumed to be 1:2 under our experimental conditions (Palade and Vergara, 1981; Rios and Schneider, 1981). The change in the molar extinction coefficient, $\Delta\epsilon(720)$, for the formation of 1 M of a 1:2 Ca:indicator complex was taken to be 1.64×10^4 M^{-1} cm^{-1}; this value was obtained by doubling the value, referred to 1 M indicator, given by Rios and Schneider (1981) and Kovacs et al. (1983*a*), and was used for measurements made with the 10-nm bandpass filter. With the 30-nm bandpass filter, $\Delta\epsilon(720)$ was determined empirically by scaling the 30-nm Ca signal to match the simultaneously recorded 10-nm Ca signal. The average scale factor from four fibers was 1.124 (range, 1.118–1.131), which gives $\Delta\epsilon(720) = 1.46 \times 10^4$ M^{-1} cm^{-1} for the 30-nm bandpass filter.

Once $[Ap]_T$ and $[CaAp_2]$ are known, free [Ca] can be calculated from the mass-action relation:

$$\frac{[Ca]\cdot([Ap]_T - 2[CaAp_2])^2}{[CaAp_2]} = K_D, \quad (1)$$

in which K_D is the apparent dissociation constant of the 1:2 Ca:antipyrylazo III complex. This equation assumes that all the antipyrylazo III is available to react normally with Ca. It also assumes that this reaction proceeds instantaneously, a condition that is not strictly correct. In a temperature-jump measurement, the relaxation time has been given as 0.18 ms at 20°C (Scarpa et al., 1978). Inside a muscle fiber containing 0.8 mM indicator, the delay of the reaction between Ca and antipyrylazo III has been estimated indirectly as 1.4 ms at 16°C (Baylor et al., 1985).

Since the stoichiometries of the principal Ca:indicator and Mg:indicator complexes are 1:2 and 1:1, respectively, the apparent dissociation constant of antipyrylazo III for Ca in the presence of Mg should be given by $K_D = (1 + [Mg]/K_{MgAp})^2 K_{CaAp_2}$, where K_{MgAp} and K_{CaAp_2} are the dissociation constants for Mg (obtained with [Ca] = 0) and Ca (obtained with [Mg] = 0). K_{MgAp} was taken to be 6.7×10^{-3} M (Rios and Schneider, 1981), and K_{CaAp_2} was taken to be the same as that obtained in a Cs glutamate calibration solution at room temperature, 2.55×10^{-8} M^2 (Kovacs et al., 1983*a*). With the concentration of free [Mg] used in the internal solution, 1 mM (Table I in Irving et al., 1987), the apparent K_D for Ca is 3.4×10^{-8} M^2; this value has been used throughout this article.

After the results in this article had been analyzed and the figures had been prepared, Hollingworth et al. (1986) published somewhat different values for calibration parameters: $K_{CaAp_2} = 3.5 \times 10^{-8}$ M^2 and $\Delta\epsilon(720) = 2.98 \times 10^4$ M^{-1} cm^{-1} at 20°C. Baylor et al. (1986) also found that, in the absence of divalent cations, antipyrylazo III can form dimers with a dissociation constant, K_{D_2}, of 4 mM. The apparent dissociation constant of antipyrylazo III for Ca should be given by $(1 + [Mg]/K_{MgAp} + 2[Ap]/K_{D_2})^2 K_{CaAp_2}$, in which [Ap] represents the concentration of free monomeric indicator. The use of the new parameters, compared with the old, decreases the value of $[CaAp_2]$ determined from a given absorbance change but increases the apparent K_D for Ca. If free [Mg] is 1 mM and the total

concentration of indicator $[Ap]_T$ is 0.3 mM, a benchmark value used later in this article, [Ap] is ~0.24 mM and the apparent K_D for Ca is 5.6×10^{-8} M^2. At this concentration of antipyrylazo III, the overall effect of using the Hollingworth et al. (1986) and Baylor et al. (1986) calibrations is to decrease the estimate of free [Ca] by 9%.

In the measurements described in this article, the λ_2 and λ_3 filters (Irving et al., 1987) were 720 and 810 nm, respectively; they had a 30-nm bandpass. Filters with a 10-nm bandpass were used in the λ_1 position, the standard filter being 550 nm. Measurements of resting and active absorbance were corrected for the intrinsic contribution as described in Maylie et al. (1987*b*), using Eqs. 1 and 2 of that article; the 810-nm absorbance change was used for the intrinsic signal in Eq. 2. Active signals were recorded using 0.625-kHz eight-pole Bessel filters. To further reduce noise in the intrinsic correction, $\Delta A(810)$ was additionally filtered by a 0.05–0.2-kHz Gaussian digital filter (Colquhoun and Sigworth, 1983; see Fig. 16*B* in Irving et al., 1987). The cutoff frequency was selected to be as low as possible without noticeably changing the waveform of the signal.

All measurements of $A(\lambda)$ and $\Delta A(\lambda)$ in this article have had the intrinsic contributions subtracted, except for the traces in Figs. 5*A* and 11*A* and some of the traces in Fig. 19.

RESULTS

Experiments were carried out on 23 fibers in Ringer's solution, using action potential stimulation, and 8 fibers in TEA solution, using the voltage-clamp technique. Table I provides information about these fibers and their electrical viability during the time course of the experiments. The results show that the fibers held up well.

Diffusion and Resting Spectrum of Antipyrylazo III in Cut Muscle Fibers

Diffusion Analysis Including Reversible Binding

Comparison of diffusion in a notched and a saponin-treated fiber. The preceding article (Maylie et al., 1987*b*) showed that arsenazo III appears to be bound to or taken up by intracellular constituents in cut muscle fibers. This article shows that antipyrylazo III behaves similarly. Throughout this article, indicator that is not free to diffuse in myoplasmic solution will be called bound indicator.

The following experiment shows that indicator binding is not caused by the saponin treatment routinely used to render the end-pool segments of cut fibers permeable to the indicator. Two fibers were dissected from the two semitendinosus muscles from the same frog. One fiber was treated with saponin and the other was notched before being exposed to 0.25 mM antipyrylazo III in the two end pools. Fig. 1*A* shows the time course of the antipyrylazo III concentration, monitored optically, in the center of each fiber in the central pool. In both the saponin-treated (circles) and notched (squares) fibers, the concentration of indicator at the optical site eventually exceeded that in the end pools by a factor of 2 or more. Thus, antipyrylazo III binds to intracellular constituents inside either a saponin-treated or a notched muscle fiber.

In Fig. 1*A*, the time course of indicator entry was slower in the notched fiber than in the saponin-treated fiber, which is consistent with the longer path length for diffusion. Fibers treated with saponin should be permeable to the indicator throughout the end-pool regions, including the region next to the Vaseline seals

(Fig. 1 in Irving et al., 1987), whereas notched fibers would be expected to admit indicator only at the notches (or cut ends 0.5–1 mm from the Vaseline seals). Accordingly, in saponin-treated fibers, the diffusion path was taken to be the distance from the edge of the Vaseline seals in the end pools to the center of the

TABLE I

Changes in Electrical Parameters during the Time Course of Experiments on Cut Muscle Fibers Containing Antipyrylazo III

(1) Fiber reference	(2) Duration of experiment	(3) Temperature	(4) Diameter	(5) Action potential	(6) Holding current	(7) r_m	(8) $r_e/(r_e + r_i)$
	min	*°C*	*μm*	*mV*	*−nA*	*MΩ·cm*	
060884.1	146	17.6–17.5	102–99	136–126	97–103	0.059–0.053	0.963–0.962
060884.2	101	19.0–18.9	118–130	134–127	65–85	0.062–0.047	0.979–0.974
061184.1	134	18.3–17.5	133–127	130–128	109–117	0.042–0.033	0.975–0.970
061184.2	137	18.0–17.5	135–133	132–124	117–145	0.040–0.036	0.970–0.959
061284.1	165	16.5–16.9	94–86	132–124	84–107	0.072–0.060	0.960–0.945
061284.2	80	17.4–17.3	94–87	130–123	144–179	0.086–0.086	0.924–0.899
061384.1	74	17.5–17.6	86–81	131–123	59–69	0.085–0.070	0.964–0.958
061484.2	177	17.5–18.0	94–82	134–129	85–97	0.090–0.069	0.967–0.954
061484.3	167	17.7–17.7	86–74	134–124	70–92	0.100–0.077	0.965–0.944
061984.2	191	18.2–17.4	112–102	134–126	66–76	0.069–0.062	0.975–0.968
062184.2	208	17.9–18.5	114–92	132–123	50–55	0.062–0.036	0.980–0.974
062284.1	187	18.5–18.5	80–69	138–135	25–29	0.090–0.070	0.981–0.975
062284.2	196	18.1–17.7	93–74	132–123	79–92	0.060–0.039	0.964–0.946
062584.1	166	17.8–17.9	104–90	131–118	75–109	0.063–0.049	0.969–0.949
062684.1	153	17.7–18.1	96–87	132–120	85–102	0.065–0.052	0.963–0.946
070584.1	125	18.1–18.3	98–96	132–127	52–53	0.085–0.052	0.972–0.973
071184.2	137	19.3–19.0	80–78	136–122	37–53	0.085–0.060	0.974–0.966
071284.1	148	17.7–18.1	94–93	132–120	44–59	0.061–0.049	0.977–0.969
092484.1	172	17.2–18.1	94–86	139–134	49–42	0.160–0.099	0.977–0.975
092484.2	156	17.3–17.7	105–109	142–132	45–62	0.135–0.067	0.975–0.979
092584.2	166	18.2–18.0	102–106	128–125	38–34	0.120–0.098	0.981–0.986
092684.1	143	16.9–16.8	78–72	136–143	41–35	0.110–0.097	0.972–0.971
101284.1	86	18.0–18.6	108–106	(VC)	97–110	0.098–0.057	0.977–0.973
101684.1	170	18.7–18.3	78–64	(VC)	23–31	0.250–0.137	0.986–0.972
101984.2	155	19.2–18.5	101–96	(VC)	26–28	0.110–0.082	0.990–0.987
111384.2	139	19.3–18.7	83–70	(VC)	40–49	0.222–0.134	0.976–0.956
111584.1	129	18.0–17.5	71–57	(VC)	24–27	0.267–0.199	0.976–0.960
111684.1	93	17.9–17.8	102–95	128–126	41–37	0.060–0.046	0.980–0.981
111684.2	131	19.6–18.9	108–95	(VC)	32–41	0.136–0.056	0.987–0.980
112184.1	126	16.8–18.1	80–71	(VC)	30–45	0.231–0.124	0.980–0.968
112184.2	134	18.5–18.1	82–75	(VC)	24–31	0.221–0.110	0.987–0.979

Column 1 gives fiber reference. Column 2 gives the duration of the experiment beginning from the time of saponin treatment or, in the case of fiber 060884.1, when notches were cut. Columns 3–8 give temperature, fiber diameter, action potential amplitude, holding current (sign reversed), r_m, and $r_e/(r_e + r_i)$; within each column, the first value was obtained ~20 min after saponin treatment and the second value was obtained at the end of the experiment. Sarcomere spacing, 3.7–4.2 μm; action potential experiments, Ringer's solution; voltage-clamp experiments (VC), TEA solution (containing 1 μM tetrodotoxin); holding potential, −90 mV.

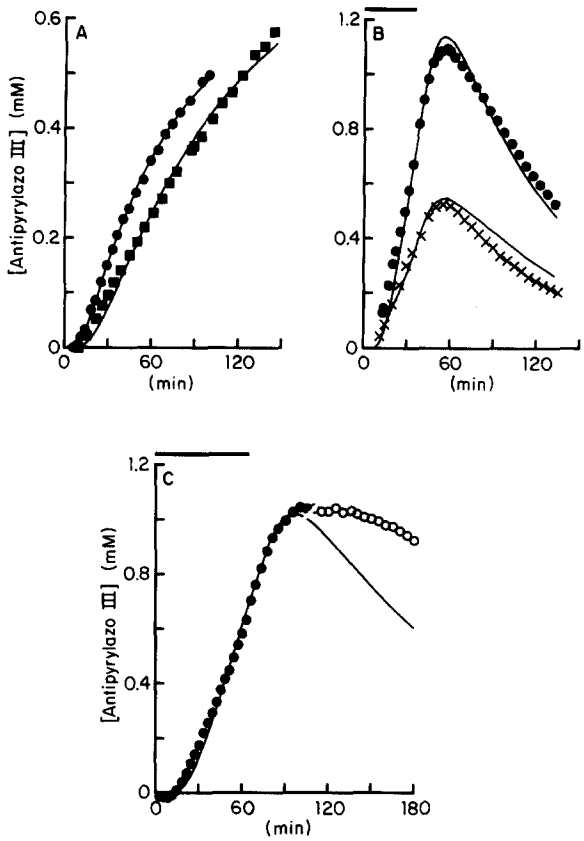

FIGURE 1. Diffusion of antipyrylazo III in cut muscle fibers. Panels *A–C* show the indicator concentration at the optical recording site plotted against time after the addition of antipyrylazo III to the end-pool solutions. The curves, except for the lower one in *B*, show least-squares fits of Eqs. 6 and 8 in Maylie et al. (1987*b*), derived from diffusion plus linear reversible binding; the fitted parameters are given in columns 4 and 5 of Table II. (*A*) Data from two fibers taken from the two semitendinosus muscles of a frog and exposed to 0.25 mM indicator for the duration of the experiment. (●) Fiber 060884.2; sarcomere length, 4.1 μm. The end-pool regions of the fiber were made permeable to antipyrylazo III by our usual saponin treatment 2 min before adding indicator to the end pools. (■) Fiber 060884.1; sarcomere length, 4.1 μm. Entry of antipyrylazo III into the end-pool regions of the fiber was facilitated by cutting two notches, one in each end-pool ~150 μm from the Vaseline seal (i.e., $X = 150$ μm in Fig. 1 of Irving et al., 1987). No saponin was used. (*B*) Data from two fibers taken from the same semitendinosus muscle and exposed to different concentrations of indicator for the same length of time, 35 min, as indicated by the horizontal bar (a convention used to indicate the duration of indicator exposure in pulsed-exposure experiments). (●) Fiber 061184.1; sarcomere length, 3.9 μm; 1 mM indicator. (×) Fiber 061184.2; sarcomere length, 3.7 μm; 0.5 mM indicator. The curve associated with the × points was obtained by scaling the ● points by 0.5 and connecting the scaled points with line segments. In both fibers, indicator was added to the end pools 2 min after saponin treatment. (*C*) Data from fiber 062284.2; sarcomere length, 4.1 μm; exposed to 1 mM indicator for 65 min. Indicator exposure began 16 min after saponin treatment. Only the filled circles were used to determine the best-fit parameters for the theoretical curve. Additional information is given in Table I.

spot used for optical recording, 550 μm. In notched fibers, the path was taken to be this distance plus the distance between the seals and the notches. In the fiber in Fig. 1*A*, this additional distance was 150 μm, so the total diffusion path was 700 μm.

The continuous curves in Fig. 1*A* represent best least-squares fits, using the diffusion path lengths given above, of Eqs. 6 and 8 in Maylie et al. (1987*b*); these equations describe diffusional movement of indicator in the presence of linear reversible binding. The best-fit values of $D/(R + 1)$, $(R + 1)$, and D (Table II) were 0.347×10^{-6} cm^2/s, 3.065, and 1.063×10^{-6} cm^2/s for the notched fiber and 0.350×10^{-6} cm^2/s, 2.555, and 0.894×10^{-6} cm^2/s for the saponin-treated fiber. D is the diffusion constant of free indicator and R is the ratio of bound to free indicator. The two sets of values are similar, which indicates that the diffusion and binding of antipyrylazo III are similar in notched and saponin-treated fibers.

In the other fibers used in this article, saponin treatment rather than notching was used to facilitate indicator entry. One advantage of the saponin method is that the path length for diffusion is made as short as possible, so that indicator enters a saponin-treated fiber more rapidly than it enters a notched fiber (Fig. 1*A*). Another advantage is that saponin treatment does not produce either the irregularities in sarcomere spacing or the distortions that normally occur near notches in a highly stretched fiber.

Effect of indicator concentration on binding. The assumption of linear (i.e., nonsaturating) binding was tested by exposing two fibers dissected from the same muscle to different concentrations of antipyrylazo III, 0.5 and 1 mM, for the same length of time, 35 min. Fig. 1*B* shows the time course of indicator concentration at the optical recording site; ● and × denote data from the 1- and 0.5-mM exposures, respectively. The curve through the ●'s is a least-squares fit of the equations for diffusion plus linear reversible binding. The curve through the ×'s was obtained by scaling the ● points by 0.5 and connecting the resulting points with line segments; the scaled curve fits the × points reasonably well. The × data were also fitted by the equations for diffusion plus linear reversible binding; the values of $D/(R + 1)$, $(R + 1)$, and D were similar to those obtained from the ● data (fibers 061184.1 and 061184.2 in Table II).

This comparison was attempted only once and the two fibers were somewhat atypical in that the indicator readily left the central region after removal from the end pools (see below). Nonetheless, the results suggest that antipyrylazo III binding is linear in the range of concentrations used in this article. This conclusion is supported by the absence of a correlation between $(R + 1)$ and the concentration of indicator in the end pools in the experiments listed in Table II*A*; the mean ± SEM values of $(R + 1)$ at the three concentrations used were 2.732 ± 0.167 (0.25 mM), 3.583 ± 0.169 (0.5 mM), and 3.026 ± 0.158 (1.0 mM).

Diffusion of indicator associated with brief periods of exposure. In the experiments in Fig. 1*B*, the internal concentration of antipyrylazo III decreased after its removal from the end pools. The time course was approximately consistent with free diffusion plus linear reversible binding, so that the theoretical curves

TABLE II

Parameters Associated with the Analysis of Antipyrylazo III Diffusion in Cut Fibers, Including Reversible Binding

(1) Fiber reference	(2) Indicator concentration	(3) Indicator exposure	(4) $D/(R+1)$	(5) $(R+1)$	(6) D
	mM	*min*	$\times 10^{-6}$ *cm²/s*		$\times 10^{-6}$ *cm²/s*
(*A*) Ringer's solution, early indicator entry					
060884.1 (1*A*, 6*A*)	0.25	144	0.347	3.065	1.063
060884.2 (1*A*, 6*A*)	0.25	99	0.350	2.555	0.894
061184.1 (1*B*, 7*A*)	1.00	35	0.258	3.656	0.943
061184.2 (1*B*, 7*A*)	0.50	35	0.289	3.145	0.909
061284.2	0.50	51	0.231	3.824	0.883
061384.1	1.00	33	0.254	3.356	0.852
061484.2	0.50	36	0.277	4.166	1.154
061484.3 (14*A*)	0.50	36	0.292	3.699	1.080
061984.2	0.25	141	0.237	2.576	0.611
062184.2	1.00	39	0.240	3.219	0.773
062284.1	1.00	65	0.164	2.617	0.429
062284.2 (1*C*, 8*A*)	1.00	65	0.158	2.947	0.466
062584.1	1.00	133	0.118	2.908	0.343
062684.1	1.00	35	0.214	3.576	0.765
070584.1 (4*A*)	1.00	41	0.261	2.882	0.752
071184.2 (3*A*)	1.00	35	0.261	3.575	0.933
092484.1	0.50	48	0.214	3.079	0.659
092484.2	0.50	50	0.162	3.583	0.581
092684.1	1.00	23	0.360	2.632	0.947
111684.1	1.00	24	0.485	1.917	0.930
Mean			0.259	3.149	0.798
SEM			0.019	0.121	0.050
(*B*) Ringer's solution, late indicator entry					
061284.1	0.50	38	0.292	2.304	0.673
071284.1	1.00	36	0.311	2.375	0.739
092584.2	1.00	42	0.283	2.282	0.646
Mean			0.295	2.320	0.686
SEM			0.008	0.028	0.028
(*C*) TEA solution					
101284.1	1.00	33	0.230	3.780	0.869
101684.1 (18*A*)	1.00	31	0.248	3.364	0.834
101984.2	1.00	36	0.223	3.047	0.679
111384.2	1.00	30	0.289	3.042	0.879
111584.1	1.00	28	0.307	2.289	0.703
111684.2	1.00	38	0.256	2.031	0.520
112184.1	1.00	27	0.332	2.695	0.895
112184.2	1.00	32	0.291	2.265	0.659
Mean			0.272	2.814	0.755
SEM			0.014	0.213	0.048

fitted the data during the entire experiment reasonably well. In all other pulsed-exposure experiments, however, the theoretical curve could not be made to fit both early and late experimental points; antipyrylazo III appeared to diffuse out of fibers more slowly than it diffused in.

Fig. 1 *C* shows a typical example. The parameters used for the theoretical curve were obtained by fitting only the early experimental points indicated by the filled circles. The curve fits these points, but not the later points (open circles), reasonably well. Another theoretical curve (not shown), obtained by fitting all the points, did not give a good fit to either the early or the late points.

Columns 4–6 of Table II list values of $D/(R + 1)$, $(R + 1)$, and D for all fibers in this article. Pulsed exposure of indicator was used in most experiments, so, except for the two fibers in Fig. 1 *B*, only the early part of the concentration time course was used for the fit, as in Fig. 1 *C*. The tabulated parameters therefore apply to the diffusion of antipyrylazo III into, rather than out of, a cut muscle fiber.

Section *A* of Table II gives values of parameters from freshly prepared cut fibers in Ringer's solution at 18°C. The average value of the apparent diffusion constant $D/(R + 1)$ was 0.259×10^{-6} cm^2/s (column 4). This value is similar to that obtained by Baylor et al. (1986) for intact fibers at 16°C, 0.21×10^{-6} cm^2/s, and somewhat smaller than the value reported by Kovacs et al. (1983*a*) for cut fibers at 6–9°C, 0.36×10^{-6} cm^2/s.

The average ratio of bound to free indicator, R, was 2.149 (Table II*A*, column 5). This value is considerably larger than the value 0.45 reported by Kovacs et al. (1983*a*). In their experiments, the temperature was 6–9°C, compared with an average temperature of 18°C in our experiments, and the duration was only long enough to allow the indicator concentration at the optical site to reach 0.7 times that in the end pools.

The average value of the diffusion constant for free indicator, D, was 0.798×10^{-6} cm^2/s (Table II*A*, column 6). This is two-thirds of the value 1.2×10^{-6} cm^2/s obtained by Kushmerick and Podolsky (1969) for the diffusion of ATP inside a skinned muscle fiber at 20°C. Since the molecular weight of ATP is ~0.7 times that of antipyrylazo III, and since the ATP measurement was done at a slightly higher temperature, 20 rather than 18°C, the two values of D seem in good agreement. Free antipyrylazo III and also arsenazo III (Maylie et al.,

---

TABLE II. (*opposite*) Column 1 gives fiber reference; the numbers and letters in parentheses refer to figures in which theoretical diffusion curves are shown. Column 2 gives the concentration of indicator used in the end pools and column 3 gives the period of time that it was present. Columns 4 and 5 give parameters associated with fitting Eqs. 6 and 8 in Maylie et al. (1987*b*) to the experimental points; column 6 gives the product of columns 4 and 5. Except for fibers 061184.1 and 061184.2 (Fig. 1 *B*), in experiments using pulsed exposure of an indicator, the data used for fitting the equations were arbitrarily limited to the time period up to and slightly past the peak so that a good theoretical fit to the early experimental points would be made (see Fig. 1 *C*). In section *A*, the indicator was added to the end pools 2–50 min (average value, 22 min) after saponin treatment or notching. In section *B*, the elapsed time was 112–127 min (average value, 121 min); in section *C*, it was 15–54 min (average value, 23 min). The average temperature was 17.9°C in *A*, 17.6°C in *B*, and 18.4°C in *C*. Additional information is given in Table I.

1987*b*) probably diffuse at similar rates inside intact, cut, and skinned fibers.

Section *C* of Table II gives values of $D/(R + 1)$, $(R + 1)$, and D from eight fibers bathed in TEA solution. The average values in columns 4–6 are not significantly different from those in section *A*, which indicates that antipyrylazo III diffusion and binding are the same with either Na or TEA in the external solution.

Diffusion Analysis Including Reversible and Irreversible Binding

In all but two experiments (Fig. 1*B*), antipyrylazo III appeared to diffuse out of a fiber less rapidly than it diffused in. Arsenazo III gave similar results. Since the time course of arsenazo III concentration could be reasonably fitted by

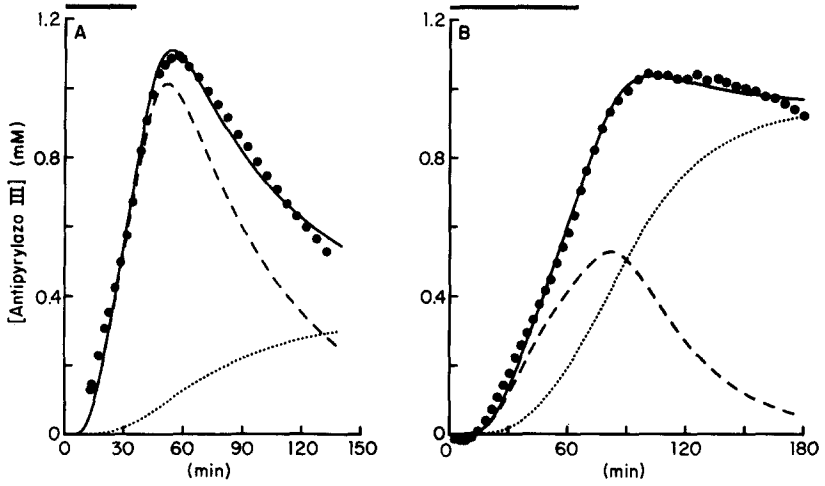

FIGURE 2. Diffusion of antipyrylazo III in cut muscle fibers with analysis based on linear reversible and irreversible binding. (*A*) Same concentration data as the filled circles in Fig. 1*B*. The continuous curve shows the best theoretical fit for diffusion plus linear reversible and linear irreversible binding (Eqs. 10 and 11 in Maylie et al., 1987*b*); the parameters are listed in columns 2, 3, and 5 of Table III. The interrupted curves show the two components of indicator, irreversibly bound (dotted) and free plus reversibly bound (dashed). (*B*) Similar to *A*, using data in Fig. 1*C*.

equations derived from diffusion plus linear reversible and linear irreversible binding (Maylie et al., 1987*b*), the same equations were tried here.

Fig. 2, *A* and *B*, shows the same experimental points that were plotted in Fig. 1, *B* (circles) and *C*, respectively. The continuous curves show the total indicator concentration calculated from Eqs. 10 and 11 in Maylie et al. (1987*b*), using parameters obtained by fitting all the experimental points. The total indicator concentration at any given time is made up of two components, one that is either free or reversibly bound (drawn as dashed curves) and another that is irreversibly bound (dotted curves). Data from the experiment in Figs. 1*C* and 2*B* are much better fitted in 2*B* than in 1*C*.

Values of fitted parameters from all the pulsed-exposure experiments are given in Table III. Sections *A* and *B* give values in Ringer's and TEA solution, respectively. Within each section, there is great variability in the values of some parameters, particularly $(R + 1)$ (column 3), D (column 4), and k (column 6). The corresponding mean values in the two sections are not significantly different.

Although curves calculated from diffusion plus linear reversible and linear

TABLE III

Parameters Associated with the Analysis of Antipyrylazo III Diffusion in Cut Fibers, Including Reversible and Irreversible Binding

(1) Fiber reference	(2) $D/(R + 1)$	(3) $(R + 1)$	(4) D	(5) $k/(R + 1)$	(6) k
	$\times 10^{-6}$ cm^2/s		$\times 10^{-6}$ cm^2/s	$\times 10^{-3}$/s	$\times 10^{-3}$/s
(*A*) Ringer's solution					
061184.1 (2*A*)	0.281	3.471	0.975	0.067	0.233
061184.2	0.305	3.034	0.925	0.029	0.089
061284.2	0.210	20.441	4.293	1.704	34.821
061384.1	0.194	24.355	4.725	1.604	39.058
061484.2	0.279	4.347	1.213	0.071	0.309
061484.3	0.288	4.134	1.191	0.131	0.543
062184.2	0.192	24.675	4.738	1.737	42.858
062284.1	0.128	22.949	2.937	1.235	28.331
062284.2 (2*B*)	0.153	4.962	0.759	0.356	1.767
062684.1	0.178	20.601	3.667	1.363	28.085
070584.1	0.267	3.562	0.951	0.322	1.146
071184.2	0.264	4.529	1.196	0.322	1.458
092484.1	0.187	4.628	0.866	0.184	0.851
092484.2	0.160	6.372	1.020	0.438	2.788
092684.1	0.302	4.815	1.454	0.504	2.426
111684.1	0.461	3.256	1.501	1.049	3.415
Mean	0.241	10.008	2.026	0.695	11.761
SEM	0.021	2.217	0.373	0.159	4.075
(*B*) TEA solution					
101284.1	0.198	17.145	3.412	1.328	22.765
101684.1	0.222	4.852	1.077	0.225	1.078
101984.2	0.180	22.851	4.113	1.613	35.331
111384.2	0.179	34.733	6.217	1.581	54.923
111584.1	0.293	4.049	1.186	0.722	2.921
111684.2	0.165	23.612	3.896	1.564	36.936
112184.1	0.336	3.830	1.287	0.604	2.315
112184.2	0.231	21.207	4.899	2.350	49.826
Mean	0.226	16.535	3.261	1.248	25.762
SEM	0.021	5.846	0.675	0.243	7.718

Column 1 gives fiber reference; the numbers and letters in parentheses refer to figures in which theoretical diffusion curves are shown. Columns 2, 3, and 5 give parameters associated with fitting Eqs. 10 and 11 of Maylie et al. (1987*b*) to the experimental points. Column 4 gives the product of columns 2 and 3, and column 6 gives the product of columns 3 and 5. Only pulsed-exposure experiments were analyzed in this table and all experimental points were used in making the fits. Additional information is given in Tables I and II.

irreversible binding fit most concentration time courses reasonably well, as in Fig. 2, the average values of D, 2.026×10^{-6} cm^2/s in section A and 3.261×10^{-6} cm^2/s in section B, seem too high for the theory to be tenable in the simple form used here. These values are similar to those associated with diffusion, along skinned muscle fibers at 20°C, of molecules much smaller than antipyrylazo III (746 mol wt); for example, $D = 2.1 \times 10^{-6}$ cm^2/s for sucrose (342 mol wt) and 3.0×10^{-6} cm^2/s for sorbitol (182 mol wt) (Kushmerick and Podolsky, 1969). We have not attempted to modify the theory to see whether good fits can be obtained with smaller, more realistic values of D.

Other Observations on Diffusion of Indicators at Late Times

This section deals with the possibility that the condition of the fiber changes during an experiment, and that this change somehow retards the movement of antipyrylazo III, after its removal from the end pools, away from the site of optical recording. Three observations provide information on this possibility.

The first observation is that fibers treated with saponin and exposed to antipyrylazo III 2 h later took up indicator as rapidly as other fibers exposed soon after treatment. The equations for diffusion plus linear reversible binding were fitted to concentration data from three fibers in which antipyrylazo III was applied after such a delay. The fitted parameters given in section B of Table II should be compared with the corresponding values in section A. The average values of $D/(R + 1)$ and D in the two sections are not significantly different. On the other hand, the average values of $(R + 1)$, 3.149 in section A and 2.320 in section B, are significantly different with $0.01 < P < 0.025$ using the two-tailed t test. These results show that saponin treatment does not wear off within 2 h. Antipyrylazo III can still enter a fiber and diffuse normally, although its ability to bind to intracellular constituents may be reduced. Consequently, the tendency of antipyrylazo III to remain inside a fiber after end-pool removal cannot be explained by a change in fiber condition unless the change can only occur if antipyrylazo III is present.

The second observation is that diffusional movement of antipyrylazo III does not appear to be influenced by action potential stimulation or exposure to the spot of white light used for the optical measurements. In one experiment, a fiber was treated with saponin, checked for normal electrical properties, and then exposed to antipyrylazo III in the end pools for 50 min. The fiber was not stimulated during either the period of exposure or the following 63 min. The indicator concentration was measured with incident 550-nm light, produced by a 10-nm bandpass filter, rather than white light; light exposure was limited to a fraction of a second once every 5 min. The time course of concentration was analyzed in the usual way and the parameters associated with diffusion plus binding, given in Table II (fiber 092484.2), are well within the range of those obtained from the other fibers. The indicator failed to leave the site of optical recording as rapidly as would be expected from the time course of its appearance.

The third observation is that the Ca indicator tetramethylmurexide (340 mol wt) always diffused out of fibers as rapidly as it diffused in (Maylie et al., 1987*a*). Thus, whatever process underlies the slow removal of antipyrylazo III does

not retard the movement of tetramethylmurexide in experiments using that indicator.

These observations suggest that the process underlying the apparent slow diffusion of antipyrylazo III at late times is little influenced by either exposure to light or electrical stimulation and fails to develop in the absence of indicator. The process could be related to binding of antipyrylazo III or possibly to some pharmacological effect.

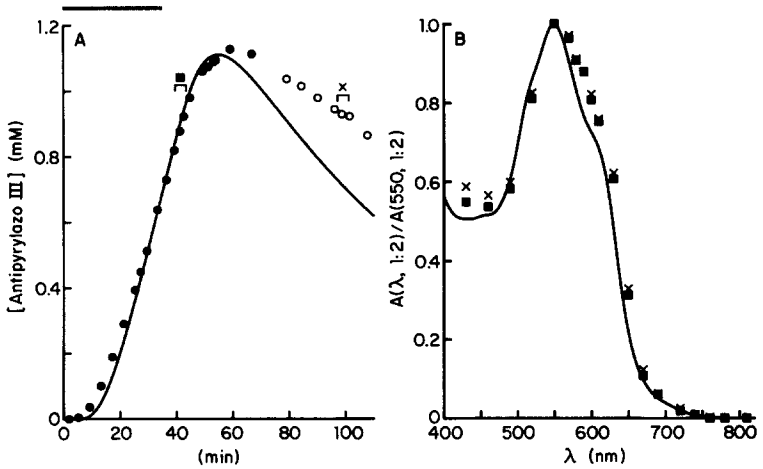

FIGURE 3. Effect of time on the wavelength dependence of antipyrylazo III absorbance in a resting cut muscle fiber. (*A*) Time course of indicator concentration. Indicator was added to the end pools 36 min after saponin treatment. The theoretical curve was calculated from Eqs. 6 and 8 in Maylie et al. (1987*b*), using the parameters given in Table II, columns 4 and 5. The resting absorbance spectrum was determined at two different times, 40 min after adding indicator to the end pools (■, with 0.82–0.98 mM indicator) and 1 h later (×, with 0.94–0.92 mM indicator). (*B*) $A(\lambda, 1{:}2)$, normalized by $A(550, 1{:}2)$, plotted against wavelength for the two runs indicated in panel *A*. The continuous calibration curve was obtained from a 100-μm cuvette that contained internal solution plus 0.6 mM antipyrylazo III, pH 6.95, and resting free [Mg] calculated to be 1 mM, 16°C. Fiber 071184.2; sarcomere length, 4.1 μm. Measurements of absorbance in this and subsequent figures, unless otherwise noted, have been corrected for intrinsic contributions.

Resting Spectrum of Antipyrylazo III

Since most of the antipyrylazo III inside a fiber is bound (Fig. 1*A*), it was of interest to determine whether the absorbance of indicator inside a fiber was different from that in free solution. Fig. 3 shows a pulsed-exposure experiment in which the resting spectrum was measured at two different times but with similar concentrations of indicator. The circles in panel *A* show the time course of concentration at the site of optical recording. The continuous curve was calculated from the equations for diffusion plus linear reversible binding, using the parameters obtained by fitting the experimental points indicated by filled

symbols. Resting absorbance spectra were measured at times marked by the ■ and the ×. The normalized spectra are shown in panel *B*. The two measurements practically superimpose, which indicates that the resting antipyrylazo III spectrum was essentially the same at early and late times. Thus, whatever process slows the diffusion of indicator at late times has little effect on the absorbance spectrum.

The continuous curve in Fig. 3*B* is a cuvette calibration using internal solution, 0.6 mM antipyrylazo III, pH 6.95, and free [Mg] calculated to be 1 mM. The muscle data are slightly red-shifted with respect to the curve, as found in cut (Kovacs et al., 1983*a*) and intact (Baylor et al., 1986) fibers. Fig. 4 shows an experiment that was similar except that the resting spectra were determined with

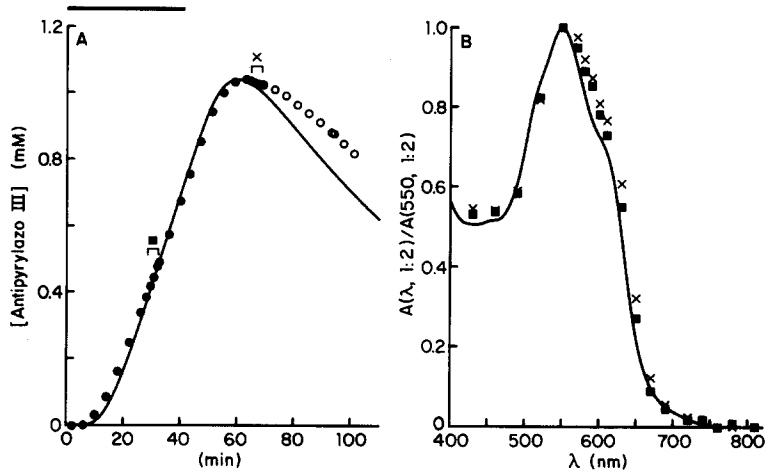

FIGURE 4. Effect of concentration on the wavelength dependence of antipyrylazo III absorbance in a resting cut muscle fiber. Same format as Fig. 3; indicator was added to the end pools 36 min after saponin treatment. ■ and × measurements were made with 0.38–0.48 and 1.04–1.02 mM indicator, respectively. Fiber 070584.1; sarcomere length, 3.7 μm.

different concentrations of antipyrylazo III. The spectrum measured with ~1 mM indicator (×'s) was slightly red-shifted ($570 \leq \lambda \leq 670$ nm) with respect to that measured with 0.4–0.5 mM indicator (squares), a consistent finding. Baylor et al. (1986) showed that the shift for $\lambda > 620$ nm is too great to be explained by uncertainties in pH or [Mg] or by a small red shift observed in cuvette calibrations and attributed to indicator dimerization. Thus, both their results and ours suggest that binding of antipyrylazo III to muscle constituents produces a small spectral shift compared with cuvette calibrations. This shift was not investigated further.

Indicator-related resting dichroism was estimated from the difference $A(550, \delta) - A(810, \delta)$. This was nearly zero in the absence of indicator and, in the 13 fibers suitable for analysis, was positive and increased approximately linearly with antipyrylazo III concentration. The ratio [antipyrylazo III–related dichroism]:

[antipyrylazo III–related $A(550, 1{:}2)$] varied from 0.025 to 0.065 with an average value of 0.042 (0.003 SEM). This value is significantly different from zero, at the level $P < 0.005$ using the two-tailed t test, and is the same as the corresponding value obtained with arsenazo III at 570 nm, 0.043 (Maylie et al., 1987*b*). Although the measurements of dichroic absorbance show too much scatter to determine the wavelength dependence reliably, the data are not inconsistent with the resting spectrum shown in Figs. 3 and 4. The resting antipyrylazo III dichroism is probably due to oriented indicator molecules.

The experiments in Figs. 3 and 4 and others (not shown) demonstrate that the resting absorbance spectrum of antipyrylazo III inside a cut fiber is similar to that inside an intact fiber (Baylor et al., 1986). The shape of the spectrum depends slightly on the antipyrylazo III concentration but not on the length of time that elapsed after either saponin treatment or exposure to indicator. If indicator binding is reversible and the factor $(R + 1)$ is constant throughout an experiment, the results are consistent with the spectrum of bound indicator being slightly red-shifted with respect to that of free indicator and with concentration having an effect on at least one of these spectra.

Optical Signals Associated with Action Potential Stimulation

Fig. 5*A* shows optical signals produced by action potential stimulation of a cut fiber containing 0.3 mM antipyrylazo III. The top trace shows the action potential and the next three traces show changes in absorbance measured simultaneously at three different wavelengths. Absorbance is expressed as a 1:2 average of the changes measured with light linearly polarized along (0° light) and perpendicular to (90° light) the fiber axis. In a cell with radial symmetry, which should hold in muscle, 1:2 averaging cancels any contributions to the absorbance signal caused by orientation or changes in orientation of indicator molecules (Baylor et al., 1982*c*). In fibers containing antipyrylazo III, dichroic absorbance changes are usually small (see below), so that 1:2 averaged traces are nearly identical to 1:1 averaged traces or traces obtained with unpolarized light.

The absorbance signal at 810 nm, a wavelength not absorbed by antipyrylazo III, shows an early sustained decrease. The waveform is typical of changes seen in the absence of a Ca indicator (Irving et al., 1987) and is therefore considered to represent the intrinsic signal.

The other two optical traces in Fig. 5*A* show additional transient components, an increase in absorbance at 720 nm and a decrease at 550 nm. This wavelength dependence is consistent with Ca complexation by antipyrylazo III (see Fig. 12). Since antipyrylazo III absorbance at 720 and 550 nm is relatively insensitive to changes in pH and free [Mg] (Scarpa et al., 1978; Baylor et al., 1982*b*), these signals should be linear combinations of two basic waveforms, the intrinsic waveform and the waveform associated with Ca complexation of the indicator (Kovacs et al., 1979, 1983*a*). It should therefore be possible to fit the 550-nm trace by a linear combination of the 720- and 810-nm traces. This was done and the bottom trace in Fig. 5*B* shows the residual, the trace obtained when the best-fit linear combination was subtracted from the 550-nm trace in Fig. 5*A*. Since

the residual is flat, which indicates a good fit, there is no reason to suspect the presence of a third waveform in any of the records.

The next step is to subtract the intrinsic component from the 550- and 720-nm traces in Fig. 5*A*. This component is assumed to have the same waveform at all wavelengths and an amplitude that varies according to λ^{-n}, as in fibers without

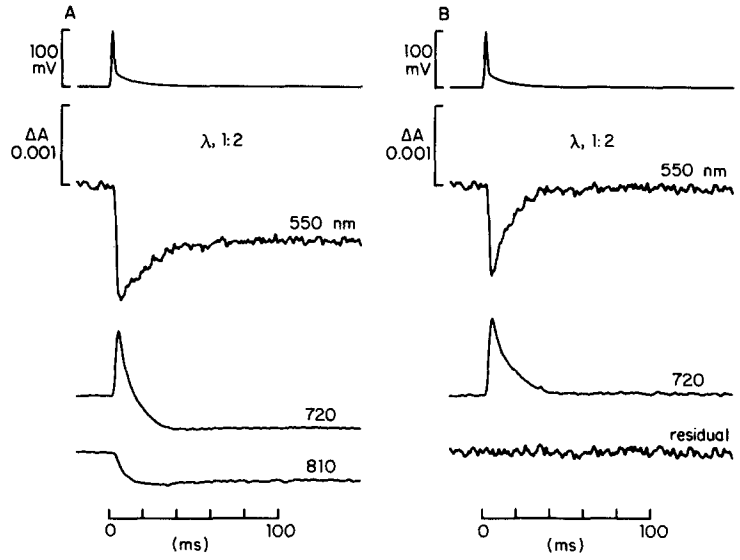

FIGURE 5. Absorbance changes produced by action potential stimulation of a cut fiber containing antipyrylazo III. (*A*) The top trace shows the action potential, attenuated by the 0.625-kHz eight-pole Bessel filter; the actual amplitude, measured on a storage oscilloscope, was 130 mV. The next three traces show uncorrected $\Delta A(\lambda, 1{:}2)$ for λ = 550, 720, and 810 nm. All signals were digitized after being filtered by 0.625-kHz eight-pole Bessel filters; the 810-nm trace was additionally filtered with a 0.2-kHz Gaussian digital filter (see Methods). (*B*) The 550-nm trace in *A* was least-squares fitted by a linear combination of the 720- and 810-nm traces in *A*. The trace labeled "residual" represents the difference between the 550-nm trace and the fitted linear combination; the scaling constants were 3.278 for 810 nm and −1.157 for 720 nm. The 550- and 720-nm traces in *B* have been corrected for the intrinsic contribution, as described in the text, using Eq. 2 of Maylie et al. (1987*b*) with n = 1.63; they therefore represent indicator-related absorbance changes. Fiber 060884.2; sarcomere spacing, 4.1 μm; temperature, 19.2°C; antipyrylazo III concentration, 0.306 mM; time after saponin treatment, 56 min. Same saponin-treated fiber as used in Fig. 1*A*. Hereafter, measurements of changes in absorbance, unless otherwise noted, have been corrected for the intrinsic contribution.

indicator (Baylor et al., 1982*a*; Irving et al., 1987). The value of n, 1.63 in this case, is evaluated from the scaling constants previously determined in fitting the 550-nm trace by the 720- and 810-nm traces. The intrinsic contributions can now be determined by scaling the 810-nm trace. The indicator-related 550- and 720-nm signals, obtained by subtraction of these contributions, are shown in *B*.

These signals should represent the change in antipyrylazo III absorbance associated with Ca complexation.

As in intact fibers (Quinta-Ferreira et al., 1983), the 0° and 90° 550- and 720-nm absorbance changes used for Fig. 5*A* had a dichroic component that depended on the presence of antipyrylazo III. In each case, the indicator-related dichroic component, determined by subtracting the 810-nm traces scaled according to λ^{-n} with $n = 1.63$, had a time course similar to that of the indicator-related 1:2 signal and an amplitude 0.06 times as large. No attempt has been made to separate the dichroic signal into components caused by either changes in the orientation of antipyrylazo III or changes in the absorbance of oriented antipyrylazo III molecules. The magnitude of the dichroic signal is sufficiently small that it has little effect on the changes in 1:2 and 1:1 absorbance; therefore, either absorbance change can be used to measure Ca.

Throughout this article, the indicator-related $\Delta A(720, 1{:}2)$ or $\Delta A(720, 1{:}1)$ signal is called the Ca signal. The intrinsic correction and the value of n were estimated using the above procedure. Although there is no easy way to test the validity of the correction in the presence of indicator, the main findings in this article do not depend critically on the correction or the exact value of n.

Effect of Antipyrylazo III Concentration and Experiment Duration on the Ca Signal

Measurements on cut fibers containing arsenazo III showed that the half-width of the Ca signal increased continually during the experimental period, regardless of whether the indicator concentration was increasing or decreasing (Maylie et al., 1987*b*). The experiments described in this section were designed to investigate this phenomenon in fibers containing antipyrylazo III. They also show the relation between the amplitude of the Ca signal and the concentration of indicator.

Comparison of results from a notched and a saponin-treated fiber. Fig. 6 shows data from the saponin-treated and notched fibers used in Fig. 1*A*. The two plots of indicator concentration vs. time are repeated in panel *A* with identification letters added. Panel *B* shows indicator-related $\Delta A(720, 1{:}2)$ or Ca signals obtained at three different times from each fiber. As the indicator concentration increased, from *a* to *c* and from *d* to *f*, the amplitude of the Ca signal increased and its duration became longer.

Fig. 6*D* shows the peak amplitude of the Ca signal plotted against indicator-related $A(550, 1{:}2)/l$, or indicator concentration. Data from the saponin-treated fiber (circles) and the notched fiber (squares) are similar, which indicates that saponin treatment of the end-pool regions had little effect on the amplitude of the Ca signal. The relation between the peak $\Delta A(720, 1{:}2)$ and the indicator concentration is parabolic in shape, as expected for a Ca:indicator stoichiometry of 1:2 (Palade and Vergara, 1981; Rios and Schneider, 1981). The peak free [Ca] was estimated by (least-squares) fitting Eq. 1 to data from the saponin-treated fiber. To minimize possible effects of indicator buffering of Ca, only experimental points taken with indicator concentrations ≤ 0.4 mM [i.e., $A(550, 1{:}2)/l \leq 10.2\ \text{cm}^{-1}$] were used for the fit. Three assumptions were made: although

some antipyrylazo III is bound to intracellular constituents, all of it can react normally (and rapidly) with Ca; the peak free [Ca] is constant and independent of indicator concentration below 0.4 mM; and the resting free [Ca] is sufficiently small that it can be taken as zero. A value of 3.05 μM was obtained for the peak

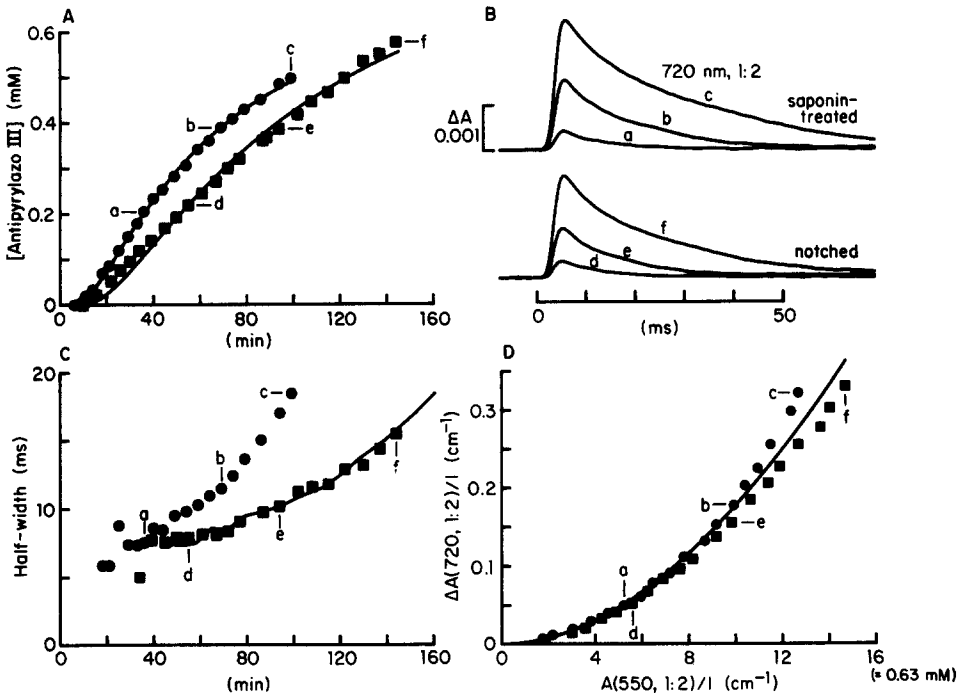

FIGURE 6. Comparison of $\Delta A(720, 1{:}2)$ signals in two cut fibers, one notched (■) and the other saponin-treated (●). Same experiment as in Fig. 1*A*. (*A*) Time course of indicator concentration with theoretical curves from Fig. 1*A*. The identification letters reference experimental points and traces in other panels of this figure. (*B*) $\Delta A(720, 1{:}2)$ signals produced by action potential stimulation. The intrinsic correction for each trace was determined using the procedure in Fig. 5; n = 1.61 (*a*), 1.60 (*b*), 1.07 (*c*), 1.35 (*d*), 1.78 (*e*), and 1.69 (*f*). The 810-nm records were digitally filtered using a 0.1-kHz Gaussian filter. (*C*) Half-width of $\Delta A(720, 1{:}2)$ plotted against time. The continuous segmented line connects the ● values of half-width replotted with time scaled by $(700/550)^2$. (*D*) Values of peak $\Delta A(720, 1{:}2)/l$ plotted against $A(550, 1{:}2)/l$ or antipyrylazo III concentration. The continuous curve was calculated from Eq. 1 using $K_D = 3.4 \times 10^{-8}$ M^2, estimated in Methods, and peak free [Ca] = 3.05 μM, obtained by fitting the experimental points from the saponin-treated fiber for antipyrylazo III concentrations ≤0.4 mM. In this and subsequent figures, a value of 0.3 cm^{-1} for $\Delta A(720, 1{:}2)/l$ recorded with the 30-nm bandpass filter corresponds to [$CaAp_2$] = 20.5 μM [using $\Delta\epsilon(720) = 1.46 \times 10^4$ M^{-1} cm^{-1} as described in Methods].

free [Ca] and this was used for the theoretical curve. A similar fit to the data from the notched fiber gave a value of 2.75 μM. This procedure for fitting $\Delta A(720)/l$ vs. $A(550)/l$ data was used throughout this article (Figs. 7*D*, 8*D*, 14*B*, and 18*D*; Table IV, column 6).

Kovacs et al. (1983*a*) carried out a similar analysis of the effect of antipyrylazo III concentration on the amplitude of the Ca signal elicited in cut fibers during voltage-clamp steps to −35 and −10 mV. They found that increasing the indicator concentration from 0.1 to 0.6 mM reduced the amplitude of free [Ca] by a factor of 4–6. Such a marked effect of indicator concentration, in the range 0.1–0.6 mM, on the amplitude of free [Ca] was never observed in our experiments (Figs. 6*D*, 7*D*, 8*D*, 14*B*, and 18*D*). Possible explanations for the difference between our and their results include (*a*) different experimental protocols (they measured free [Ca] at fixed times after voltage-clamp depolarization; we measured peak values after either action potential stimulation or brief voltage-clamp depolarization), (*b*) different temperatures (they used 6–9°C; we used 17–19°C), and (*c*) differences in fiber condition.

Fig. 6*C* shows the half-width of the Ca signal plotted against time after the addition of the indicator to the end pools. In both fibers, the half-width progressively increased but the effect developed more rapidly in the saponin-treated fiber (circles) than in the notched fiber (squares). A similar slowing of the Ca signal in cut fibers has been found by Kovacs et al. (1983*a*), who used antipyrylazo III in voltage-clamp experiments on notched fibers, and by us (Maylie et al., 1987*b*), using arsenazo III in action potential experiments on saponin-treated fibers. It does not occur, however, in intact fibers or in cut fibers neither notched nor treated with saponin that have 1–2-mm segments in the end-pool regions (Maylie et al., 1987*b*).

A possible explanation for the increase in half-width is that the internal concentration of some substance in a saponin-treated or notched cut fiber changes as a result of longitudinal diffusion, either into the fiber from the end-pool solution (for example, indicator molecules) or out of the fiber into the end-pool solution (for example, intrinsic Ca buffers or factors required for the normal operation of the sarcoplasmic reticulum Ca pump). If this explanation is correct, the effect should develop more slowly in the notched fiber, owing to the greater diffusion distance involved, than in the saponin-treated fiber. To make a quantitative comparison of the two time courses, the time after indicator exposure in the saponin-treated fiber (circles) should be multiplied by the ratio of diffusion distances squared, $(700/550)^2$. The continuous curve in Fig. 6*C* shows the ● data scaled in this way and connected with line segments. It provides a good fit to the ■ data. This agreement is consistent with the idea that the increase in half-width is due to changes in the internal concentration(s) produced by diffusion along the inside of the fiber.

Results obtained with pulsed indicator exposure. Fig. 7 shows results from the two fibers used in Fig. 1*B*; one fiber was exposed briefly to 1 mM antipyrylazo III (circles) and the other fiber, from the same muscle, to 0.5 mM (×'s). The format is similar to that in Fig. 6. Panel *A* repeats the plots of time course of indicator concentration in Fig. 1*B*. Panel *B* shows Ca signals obtained at three different times from each fiber; the traces from the 0.5-mM experiment have been plotted at twice the vertical gain used for the 1-mM experiment. Signals *a* and *d* were taken as indicator concentration was increasing, *b* and *e* when it had reached a peak, and *c* and *f* when it was decreasing. The concentration of indicator was approximately the same in runs *a* and *c*; the peak amplitudes of

the Ca signals were almost equal but the durations were different. The comparison of traces *d* and *f* is similar.

Panel *D* shows the peak amplitude of the Ca signal plotted against antipyrylazo III concentration. The ●'s (1 mM) and ×'s (0.5 mM) represent data taken as the indicator concentration was increasing; the ■'s and +'s represent data taken when the concentration was decreasing. For each fiber, it is clear that the effect of the indicator concentration on the Ca signal amplitude was reversible. Also, in the range of overlapping indicator concentrations, 6 $cm^{-1} \leq A(550, 1{:}2)/l \leq 13$ cm^{-1}, the data from both fibers are similar. The curve is plotted from Eq. 1, using peak free [Ca] = 4.86 μM determined by fitting the ● data for indicator concentrations ≤0.4 mM.

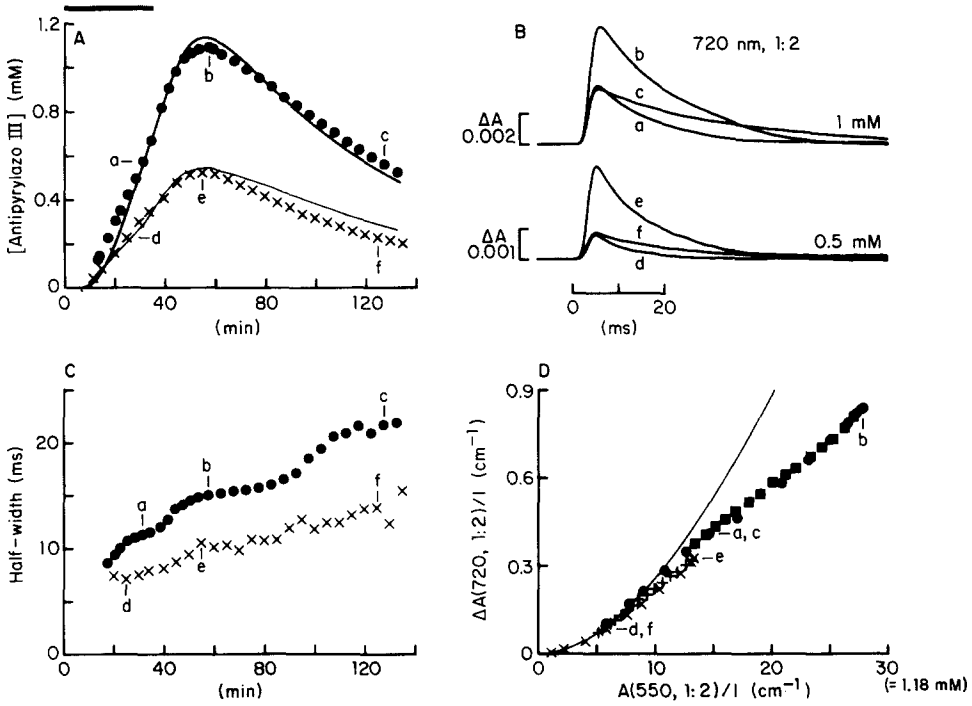

FIGURE 7. Comparison of $\Delta A(720, 1{:}2)$ signals in two fibers, one exposed to 0.5 mM and the other to 1 mM indicator. Same experiment as illustrated in Fig. 1*B*. Same format as Fig. 6. The symbols ● and ■ refer to the 1-mM experiment; × and + refer to the 0.5-mM experiment. (*A*) Indicator concentration plotted against time. The data and theoretical curves are from Fig. 1*B*. (*B*) $\Delta A(720, 1{:}2)$ signals after action potential stimulation; the intrinsic corrections used n = 1.61 (*a*), 0.16 (*b*), 0.79 (*c*), 0.12 (*d*), 1.22 (*e*), 0.96 (*f*), and a 0.1-kHz digital Gaussian filter on the 810-nm traces. (*C*) Half-width of the $\Delta A(720, 1{:}2)$ signals plotted against time. (*D*) Peak $\Delta A(720, 1{:}2)/l$ plotted against $A(550, 1{:}2)/l$ or antipyrylazo III concentration. The theoretical curve was calculated from Eq. 1 with [Ca] = 4.86 μM, obtained by fitting the ● data for antipyrylazo III concentrations ≤0.4 mM. In *D*, the symbols ● and × plot data obtained when indicator concentration was increasing; ■ and +, when concentration was decreasing.

Although the curve in Fig. 7*D* provides a good fit to data at indicator concentrations ≤0.4 mM, it lies above the points at larger concentrations. This deviation was usually observed at high concentrations of indicator and was the reason for limiting estimates of peak free [Ca] to experimental points obtained with indicator concentrations ≤0.4 mM. Several factors may contribute to this deviation: for example, Ca buffering by the indicator (Kovacs et al., 1983*a*) or formation of dimers of antipyrylazo III (Baylor et al., 1986; Hollingworth et al., 1986), which would increase its apparent dissociation constant for Ca (see Methods).

Fig. 7*C* shows Ca signal half-widths plotted against time. In each fiber, the duration of the Ca signal became longer as the experiment progressed, both during the early period when the indicator concentration was increasing and later when it was decreasing. The longer duration is due primarily to a slowing of the decay phase of the signal. The time course of the rising phase was almost constant; for example, the time to half-peak occurred 3.12 ms after that of the action potential in *a* and 3.03 ms after that of the action potential in *c*. A similar relative invariance of the time course of the rising phase was observed in the experiment in Fig. 6 and in other experiments, described below, which showed increases in half-width.

The increases in half-width in Fig. 7*C* were not accompanied by any major alteration in the electrical condition of the fibers (Table I, columns 5–8, fibers 061184.1 and 061184.2). In each fiber, the amplitude of the action potential decreased slightly but its half-width remained constant. The most noticeable change was in the afterpotential (not shown); at the end of the two experiments, its initial magnitude was 4–5 mV smaller than at the beginning and the time constant of the exponential phase of decay had decreased from ~10 to 6–7 ms. This reduction in afterpotential abbreviates the period of membrane depolarization, which in turn would be expected to decrease, not increase, the half-width of the Ca signal.

The increase in the duration of the Ca signal was more marked in the fiber exposed to 1 mM indicator (circles) than in the one exposed to 0.5 mM (×'s). Two explanations for this difference seem possible: an effect of indicator concentration, as well as time, on Ca transient duration or a difference in fiber properties (although the two fibers came from the same muscle).

The experiments in Fig. 7 show that the progressive increase in the Ca signal half-width is not due solely to an increase in the indicator concentration, which is consistent with the idea presented in the preceding section (Fig. 6) that it may be due to changes in the concentration of diffusible substances other than antipyrylazo III. Another possible explanation, however, would be a progressive change in the kinetics of the reaction between Ca and indicator. For example, antipyrylazo III might gradually become irreversibly bound (Fig. 2*A*) and Ca might dissociate slowly from such bound molecules. It is difficult to reconcile this explanation with the following observations: (*a*) the time course of the rising phase of the Ca signal did not change during the experiment; (*b*) the relation between the peak amplitude of the Ca signal and the indicator concentration was reversible (Fig. 7*D*); and (*c*) the time course of the falling phase of the Ca signal was not the sum of two distinct waveforms, a rapidly decaying waveform associ-

ated with Ca leaving nonirreversibly bound indicator and a more slowly decaying waveform associated with Ca leaving irreversibly bound indicator.

In Fig. 7, antipyrylazo III rapidly left the optical recording site after end-pool removal. Fig. 8 shows results from the experiment in Fig. 1 *C*, in which indicator left the optical site rather slowly. Panel *A* shows the time course of indicator concentration; the theoretical curve was obtained by fitting the filled circles.

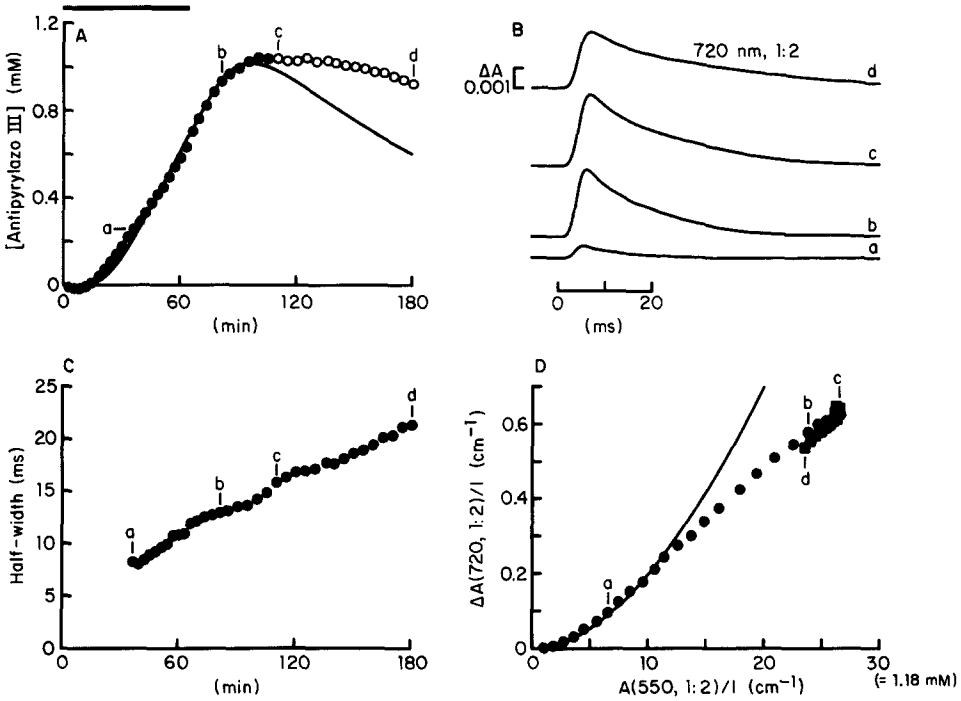

FIGURE 8. $\Delta A(720, 1{:}2)$ signals in a pulsed-exposure experiment in which indicator left the site of optical recording rather slowly. Same experiment as in Figs. 1 *C* and 2 *B*. Same format as Figs. 6 and 7. (*A*) Indicator concentration plotted against time. The data and theoretical curve are from Fig. 1 *C*. (*B*) $\Delta A(720, 1{:}2)$ signals after action potential stimulation; the intrinsic corrections used $n = 0.42$ (*a*), 0.69 (*b*), 0.93 (*c*), 1.23 (*d*), and a 0.1-kHz digital Gaussian filter on the 810-nm traces. (*C*) Half-width of the $\Delta A(720, 1{:}2)$ signals plotted against time. (*D*) Peak $\Delta A(720, 1{:}2)/l$ plotted against $A(550, 1{:}2)/l$ or indicator concentration. The theoretical curve was calculated from Eq. 1 using [Ca] = 3.58 μM, determined by fitting the ● data for antipyrylazo III concentrations ≤0.4 mM. ● and ■ denote, respectively, periods of increasing and decreasing concentrations of indicator.

Panel *B* shows Ca signals recorded at four different times. The amplitude of the signals increased from *a* to *b* to *c*, as the indicator concentration increased, and then decreased from *c* to *d* as the concentration gradually fell. The duration of the signals, however, progressively increased from *a* to *d*.

In Fig. 8 *D*, the peak amplitude of the Ca signal is plotted against antipyrylazo III concentration, using circles and squares for data obtained when the concen-

tration was increasing and decreasing, respectively. Although the indicator left the optical site only slowly, the relation between peak amplitude of the Ca signal and the indicator concentration was fairly reversible, which suggests that the availability of indicator for Ca complexation was little changed. The curve is drawn from Eq. 1 with peak [Ca] = 3.58 μM. As in Fig. 7*D*, at a high indicator concentration, the experimental points lie below the theoretical curve. Fig. 8*C* shows a plot of half-width against time. The duration of the Ca signal increased continually throughout the experiment.

Fig. 9*A* shows the half-width plotted against time from nine pulsed-exposure experiments in which the half-widths were monitored when the indicator was

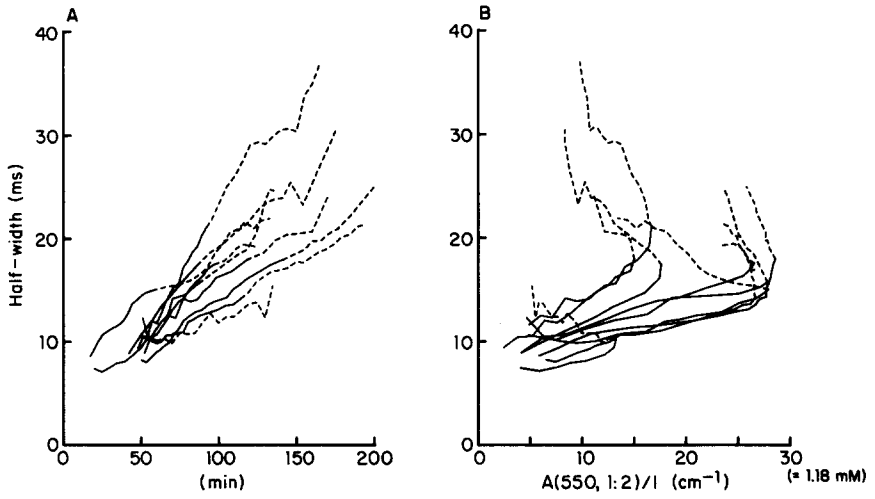

FIGURE 9. ΔA(720, 1:2) half-widths obtained from nine cut fibers after pulsed exposure to antipyrylazo III, action potential stimulation. Only data from fibers that survived for a long time after indicator removal were used for this figure. (*A*) Half-widths plotted as a function of time after saponin treatment. (*B*) Half-widths plotted against A(550, 1:2)/l or indicator concentration. In both panels, the continuous line segments connect experimental points obtained early, when the indicator concentration was increasing; the dashed line segments connect points obtained later, when the concentration was decreasing. The measurements of absorbance in one fiber, studied with mode 2 recording, were 1:1 averages.

both entering and leaving the optical recording site. Continuous line segments connect experimental points obtained when the indicator concentration was increasing; the dashed line segments connect later points. In every experiment, the duration of the Ca signal increased progressively with time.

Fig. 9*B* shows the same half-width data plotted against the concentration of indicator. In every fiber, the relation between the half-width and the concentration was not single-valued. This shows that the increase in the half-width cannot be due solely to a reversible effect of antipyrylazo III such as its Ca-buffering capacity. Rather, the increase must be related to the duration of the experiment and changes in the physiological condition of the fiber.

Properties of Ca Signals Recorded with Small Concentrations of Antipyrylazo III

The preceding results suggest that the Ca signal recorded early in an experiment, with <0.4 mM antipyrylazo III inside the fiber, provides the best estimate of the waveform of free [Ca] in a minimally perturbed cut fiber. Fig. 10 examines the relation between the half-width of the Ca signal and the antipyrylazo III concentration during indicator entry. The continuous line segments connect points obtained in 18 experiments in which antipyrylazo III was added soon after saponin treatment or, in the case of fiber 060884.1, after notching. All the

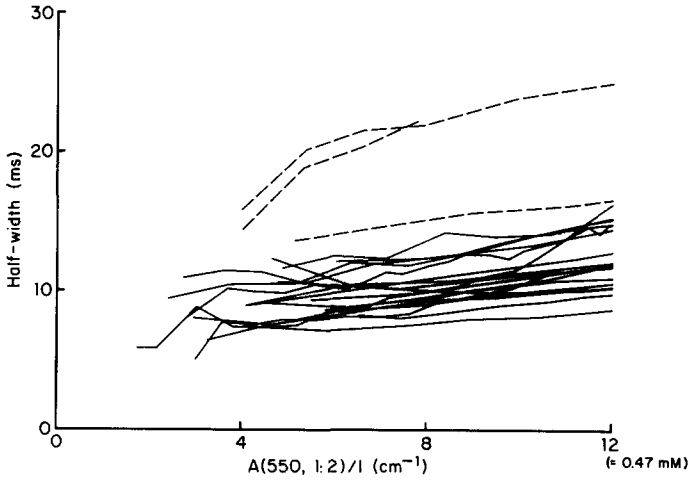

FIGURE 10. ΔA(720, 1:2) half-widths plotted against A(550, 1:2)/l early during antipyrylazo III entry into cut fibers, action potential stimulation. Continuous line segments connect experimental points from 18 of the 20 fibers listed in Table II*A*; fiber 062684.1 was not used because the intrinsic signal was too large to allow reliable correction and fiber 092484.2 was not used because it was not stimulated during indicator entry. In 2 of the 18 fibers, mode 2 was used and the absorbance measurements represent 1:1 averages. In the 18 experiments represented by continuous line segments, indicator was added to the end pools 2–50 min after saponin treatment; average temperature, 17.9°C. In three experiments, indicated by dashed line segments, indicator was added 112–127 min after saponin treatment (Table II*B*); average temperature, 17.6°C.

curves show the same trend. The half-width increased slightly as the indicator diffused into the optical recording site; this increase can be attributed to either time or indicator concentration or both.

The dashed lines in Fig. 10 are from three fibers treated with saponin ~2 h before adding indicator. These 3 curves lie above the other 18, which shows that the process(es) responsible for the increase in half-width can develop in the absence of indicator.

Column 5 of Table IV gives half-widths obtained with 0.3 mM antipyrylazo III, from the same 18 fibers represented by continuous line segments in Fig. 10. The average value was 10.1 ms. This average half-width was measured 58 min

after saponin treatment (average value in column 2) or 36 min after the addition of indicator to the end pools (average value in column 3).

Column 4 of Table IV gives the delay between the rising phase of the action potential and that of $\Delta A(720)$, estimated as the interval between the respective times to half-peak. Since the 0.625-kHz eight-pole Bessel filters shift the times to half-peak of both signals by approximately the same amount, the reciprocal

TABLE IV

Parameters Associated with $\Delta A(720)$ Signals Recorded with 0.3 mM Antipyrylazo III

(1) Fiber reference	(2) Time after saponin treatment	(3) Time after indicator	(4) Time to half-peak	(5) Half-width	(6) Peak free [Ca]
	min	*min*	*ms*	*ms*	*μM*
060884.1	74	72	2.92	8.43	2.75
060884.2	56	54	3.24	9.91	3.05
061184.1	22	20	3.07	9.50	4.86
061184.2	32	30	3.11	7.55	3.85
061284.2	36	34	3.23	8.91	3.82
061384.1	26	24	2.88	8.84	3.09
061484.2	52	26	3.04	11.58	3.12
061484.3	62	27	3.00	12.05	3.25
061984.2	126	76	3.98	10.96	2.88
062184.2	59	26	2.99	10.04	2.94
062284.1	71	42	2.76	8.55	3.30
062284.2	55	39	3.15	8.78	3.58
062584.1	87	54	3.83	12.20	2.99
070584.1	60	24	2.93	10.03	2.83
071184.2	57	21	2.64	9.90	2.15
092484.1	77	43	2.94	12.39	2.31
092684.1	54	18	2.45	12.29	2.41
111684.1	36	17	3.13	9.82	2.81
Mean	58	36	3.07	10.10	3.11
SEM			0.09	0.35	0.15

Column 1 gives fiber reference. Column 2 gives the time that elapsed from saponin treatment or, in the case of fiber 060884.1, notching to the measurement used for columns 4 and 5. Column 3 gives the time from the application of indicator to the end pools to the measurement. Column 4 gives the interval between the time to half-peak of the action potential and the time to half-peak of the indicator-related $\Delta A(720, 1{:}2)$ or $\Delta A(720, 1{:}1)$ signal. Column 5 gives the half-width of the $\Delta A(720, 1{:}2)$ or $\Delta A(720, 1{:}1)$ signal. Column 6 gives peak free [Ca]. Each value in columns 4 and 5 was determined from a $\Delta A(720)$ signal obtained with ~0.3 mM indicator (range, 0.289–0.320 mM). Each value in column 6 was determined by fitting Eq. 1 to the peak values of $\Delta A(720)$ obtained with antipyrylazo III concentrations $\leq$0.4 mM; all the indicator was assumed to be able to react normally with Ca and resting [Ca] was set to zero. Each value in column 6 is close to that calculated from the 0.3 mM antipyrylazo III $\Delta A(720)$ trace used for columns 4 and 5; these values are given in Table VI, column 4. The average temperature was 17.9°C.

of the cutoff frequency (Irving et al., 1987), the temporal separation is determined rather accurately. On average, the Ca signal reached its half-maximal value 3.07 ms after that of the action potential (average temperature, 18°C).

Column 6 of Table IV gives peak free [Ca]. The values were determined by fitting Eq. 1, assuming that all the antipyrylazo III was able to react with Ca, to data obtained with antipyrylazo III concentrations ≤0.4 mM. The average value of peak free [Ca], 3.11 μM, would require that, at an indicator concentration of 0.3 mM, 7.4 μM Ca be complexed. This represents a very small buffering of the total Ca release, which is likely to be 150–350 μM (see below), associated with a single action potential.

Wavelength Dependence of Antipyrylazo III Signals

Fig. 11 shows changes in 1:2 absorbance recorded at various wavelengths after action potential stimulation; panels *A* and *B* show traces that have not been corrected and have been corrected, respectively, for the intrinsic contribution. These traces are similar to those from intact fibers (Baylor et al., 1982*b*, 1983*b*). The indicator-related signals (*B*) show at least two distinct components: an early change, best seen in the 550-, 650-, and 720-nm signals, with a wavelength dependence consistent with Ca complexation by indicator, and a maintained change, best seen in the 590-nm signal, consistent with an increase in pH or free [Mg] (Baylor et al., 1982*b*). Properties of the maintained signal will be described in a later article.

Fig. 12 shows the wavelength dependence of the early change in antipyrylazo III absorbance. Each experimental point was obtained by scaling the indicator-related $\Delta A(720, 1{:}2)$ signal, such as shown in Fig. 11*B*, to fit the simultaneously recorded $\Delta A(\lambda, 1{:}2)$ signal. Only the early time course, up to about two-thirds of the peak of the 720-nm signal, was used for the fits; this minimizes contributions from the more slowly developing maintained signal. The continuous curve is a cuvette Ca-difference spectrum from Baylor et al. (1982*b*); it shows the changes in absorbance expected for the formation of complexes of Ca:indicator with a predominant stoichiometry of 1:2. The points are in reasonable agreement with the curve, similar to observations in intact fibers (Baylor et al., 1982*b*, 1983*b*). Some of the small discrepancies may arise from differences in pH or free [Mg] between myoplasm and the cuvette solution or from the difference between the muscle resting spectrum and the cuvette resting spectrum (Figs. 3 and 4).

Active Dichroic Signals

Quinta-Ferreira et al. (1983) reported that intact fibers containing antipyrylazo III have an indicator-related dichroic signal. This early signal has a time course and spectrum similar but not identical to those of the Ca signal. As mentioned in the description of Fig. 5, cut fibers have a similar antipyrylazo III–related dichroic signal (not shown). At 720 nm, its waveform is qualitatively similar to that of the $\Delta A(720, 1{:}2)$ Ca signal; it is slightly slower, however, and at 18°C reaches a peak value 1–4 ms later than the Ca signal. The ratio of the peak amplitudes of the dichroic and Ca signals, $\Delta A(720, \delta)/\Delta A(720, 1{:}2)$, is relatively independent of the indicator concentration. In the saponin-treated fiber used in

Fig. 6, for example, the ratio was 0.060 in *a*, 0.065 in *b*, and 0.058 in *c*. In three other fibers analyzed, the ratio varied from 0.05 to 0.09. The spectrum of $\Delta A(\lambda, \delta)$ is similar to that of the Ca signal, but since the waveform of the dichroic signal varies somewhat with wavelength, it is difficult to make the comparison quantitative.

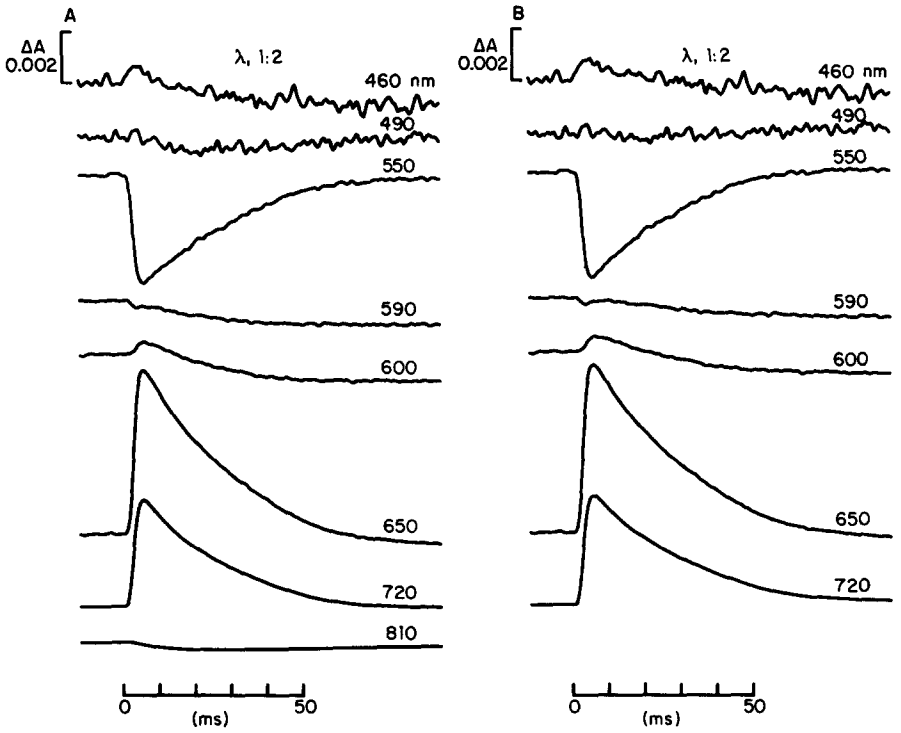

FIGURE 11. $\Delta A(\lambda, 1{:}2)$ traces obtained at different wavelengths after action potential stimulation. (*A*) Uncorrected $\Delta A(\lambda, 1{:}2)$. The 720- and 810-nm records were obtained with 30-nm bandpass filters; all other records were taken with 10-nm bandpass filters. The 810-nm record has been filtered by a 0.1-kHz Gaussian digital filter. (*B*) 1:2 averages corrected for the intrinsic signal using $n = 0.38$. Fiber 061384.1; sarcomere spacing, 4.2 μm; antipyrylazo III concentration, 1.012–1.091 mM; time after saponin treatment, 56–71 min.

Comparison of Changes in $\Delta A(720)$ and Changes in Retardation

The amplitude and half-width of both Ca (Maylie et al., 1987*b*; this article) and retardation (Irving et al., 1987) signals can change during the time course of a cut fiber experiment. Since the retardation signal may be caused by the increase in myoplasmic [Ca] (Suarez-Kurtz and Parker, 1977), we wanted to compare the two signals in the same experiment. The optical traces shown thus far in this article were obtained with mode 1 recording. This mode measures only absorb-

ance, including linear dichroism. To compare changes in absorbance and retardation, it is necessary to use mode 2 recording (Irving et al., 1987).

Fig. 13 shows Ca and retardation signals recorded simultaneously after action potential stimulation at different times and with different concentrations of antipyrylazo III inside the fiber (Fig. 14*A*). Panel *A* shows an action potential and six traces of antipyrylazo III–related $\Delta A(720, 1{:}1)$. Trace *a* was taken before the indicator was added to the end pools. The absence of a signal shows that the

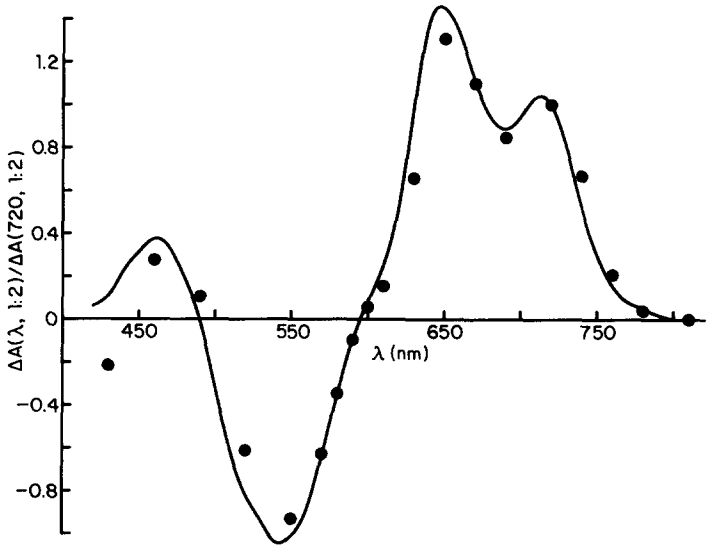

FIGURE 12. Wavelength dependence of the early antipyrylazo III absorbance change, from the experiment in Fig. 11*B*. Each experimental point gives the scale factor obtained by fitting the $\Delta A(\lambda, 1{:}2)$ trace by the simultaneously recorded $\Delta A(720, 1{:}2)$ trace, previously multiplied by 1.147 to give the amplitude expected for a 10-nm bandpass filter; the factor 1.147 was determined from the magnitude of the 720-nm absorbance change measured with the 10-nm bandpass filter divided by that measured simultaneously with the 30-nm bandpass filter. The early part of the absorbance change, up to approximately two-thirds of the peak of the $\Delta A(720, 1{:}2)$ trace, was used for each fit. The continuous curve is a Ca-difference spectrum taken from Fig. 10 of Baylor et al. (1982*b*). The calibration solution contained 150 mM KCl, 2 mM Mg, 70 μM antipyrylazo III, and either 0 or 0.25 mM free [Ca]; pH 6.9.

intrinsic correction worked well. Traces *b*–*d* were taken as the indicator diffused to the optical recording site and reached a peak concentration; *e* and *f* were taken as the concentration decreased. The magnitude of the Ca signal varied as expected with the antipyrylazo III concentration and the half-width increased monotonically throughout the experiment.

Fig. 13*B* shows 810-nm retardation signals. These also changed during the experiment. The peak amplitude increased continually from *a* to *d*, and then

remained relatively constant from *d* to *f*. The half-width progressively increased from *a* to *f*. In contrast to these changes in $\Delta R(810)$, resting retardation remained nearly constant; it gradually increased from 152 nm in *a* to 160 nm in *f*.

Fig. 14*B* shows the relation between the peak amplitude of the Ca signal and the concentration of antipyrylazo III. The two symbols refer to data obtained

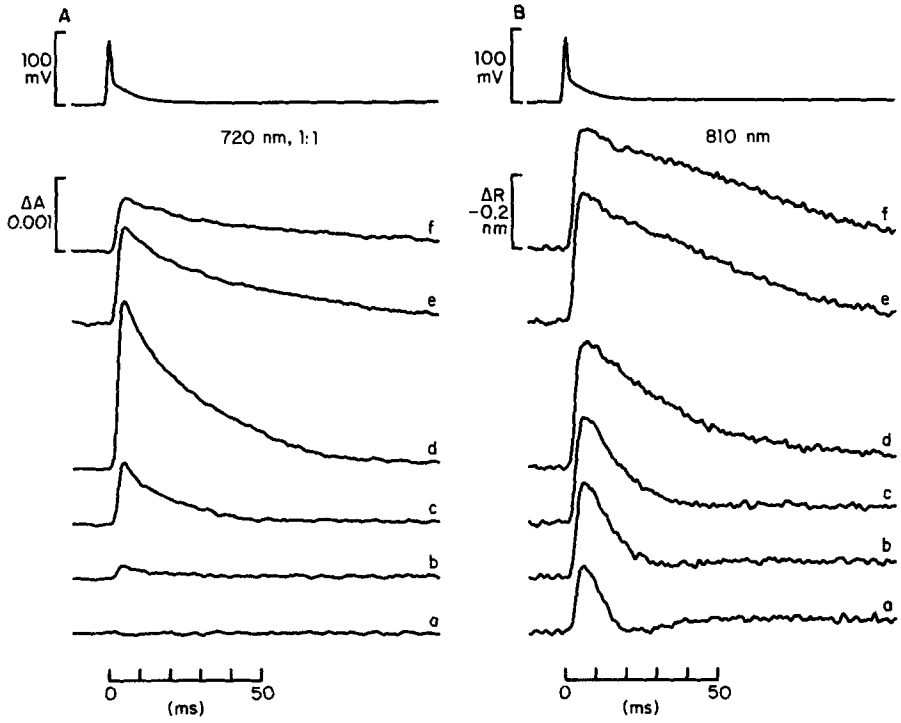

FIGURE 13. Records of $\Delta A(720, 1{:}1)$ and $\Delta R(810)$ taken at different times in a pulsed-exposure experiment. (*A*) The top trace shows an action potential; the actual peak magnitude varied from 134 to 124 mV during the experiment (Table I). The next six traces show $\Delta A(720, 1{:}1)$ obtained with mode 2 recording (Fig. 3 in Irving et al., 1987). The intrinsic contribution was subtracted in the usual way using a 0.1-kHz digital Gaussian filter for the 810-nm records; n = 0.36 (*a*), 1.26 (*b*), 1.31 (*c*), 1.74 (*d*), 1.48 (*e*), and 0.87 (*f*). (*B*) Action potential and $\Delta R(810)$ traces determined from the same mode 2 records used in *A*. In this and subsequent figures, the ΔR traces have been plotted with inverted polarity. Resting retardation (averaged at 550, 720, and 810 nm) = 152 (*a*), 154 (*b*), 155 (*c*), 157 (*d*), 159 (*e*), and 160 (*f*) nm. The identification letters apply to Figs. 13–15. Fiber 061484.3; sarcomere spacing, 3.8 μm.

when the indicator concentration was increasing (circles) and then decreasing (squares). In this experiment, the indicator left the optical site fairly rapidly after end-pool removal (Fig. 14*A*). The effect of the indicator concentration on the amplitude of the Ca signal was reasonably reversible. The continuous curve was obtained from Eq. 1 and constant peak [Ca] = 3.25 μM, the value obtained by

fitting the ● data for indicator concentrations ≤0.4 mM. These results are similar to those obtained with mode 1 recording (shown above), which indicates that the fiber was typical.

Fig. 15*A* shows the peak free [Ca], calculated from Eq. 1, and peak retardation plotted against time after the application of antipyrylazo III; the indicator concentration is shown at the bottom. The peak [Ca] (circles) decreased as antipyrylazo III diffused into the optical recording site, and then increased and later decreased as indicator diffused away. Peak retardation (×'s), on the other hand, steadily increased during the period before indicator was added (time < 0) and continued to increase past the time when the indicator concentration had

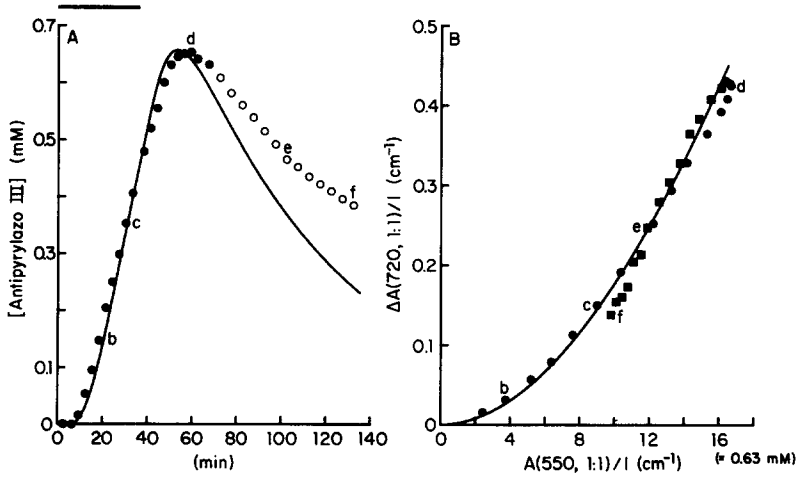

FIGURE 14. (*A*) Antipyrylazo III concentration plotted against time, from the experiment in Fig. 13. Indicator was added to the end pools 35 min after saponin treatment. The theoretical curve was calculated from Eqs. 6 and 8 of Maylie et al. (1987*b*) using the parameters given in columns 4 and 5 of Table II. (*B*) $\Delta A(720, 1{:}1)/l$ from the same experiment plotted against $A(550, 1{:}1)/l$ or indicator concentration. ● and ■ denote experimental points obtained, respectively, when indicator concentration was increasing and decreasing. The theoretical curve was calculated from Eq. 1 using [Ca] = 3.25 μM, obtained by fitting the ● data for antipyrylazo III concentrations ≤0.4 mM.

reached a maximum. The peak value between *d* and *e* was twice that in *a*. This experiment shows that there is not a constant relation between the peak of the retardation signal and the peak free [Ca] estimated with antipyrylazo III.

Fig. 15*B* shows half-widths of the Ca (circles) and retardation (×'s) signals plotted against time after exposure to antipyrylazo III. The earliest measurements of retardation half-width gave a relatively constant value just under 10 ms. Later, the duration of both Ca and retardation signals increased, with the half-width of the retardation signal always being greater than that of the Ca signal.

In six other experiments, five with and one without indicator, the amplitude

and half-width of the retardation signal progressively increased during the experiment (see Fig. 15 in Irving et al., 1987). The variation shown in Fig. 15 is typical of that usually observed in cut fibers and therefore cannot be attributed solely to the presence of antipyrylazo III.

Changes in ΔA(720) and Retardation during Repetitive Stimulation

Fig. 16 shows the results of a repetitive stimulation experiment. Panels *A* and *B* show the same traces plotted on two different time bases. The top pair of traces shows 1 and 10 action potentials, the middle pair shows the associated Ca signals,

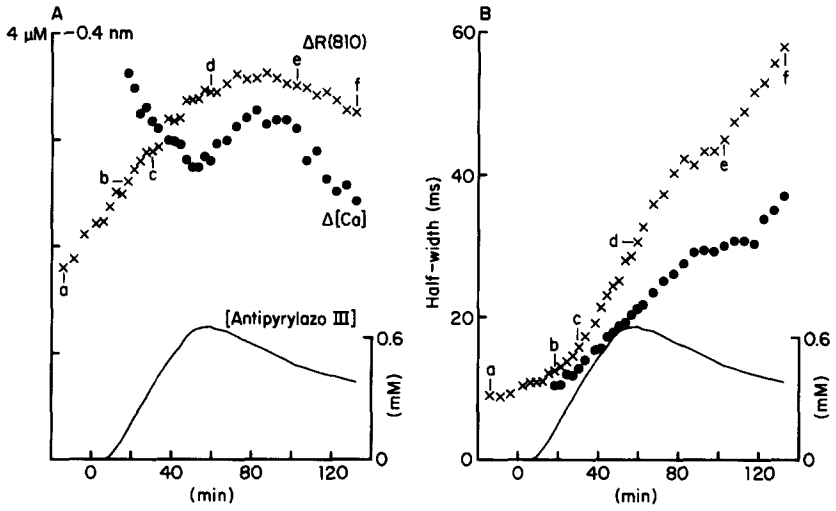

FIGURE 15. Peak values and half-widths of Ca and retardation signals. (*A*) Peak values of free [Ca] (●) and retardation (×) plotted as a function of time; $t = 0$ corresponds to the time that indicator was added to the end pools, 35 min after saponin treatment. [Ca] was calculated from Eq. 1 assuming that all the antipyrylazo III was available to react normally with Ca. (*B*) Half-widths of $\Delta A(720, 1{:}1)$ (●) and $\Delta R(810)$ (×) plotted as a function of time. The curve in the lower part of each panel shows straight line segments connecting antipyrylazo III concentration points taken from Fig. 14*A*.

and the bottom pair shows the retardation signals. Similar to results in intact fibers (Quinta-Ferreira et al., 1984*a*), the Ca signal did not summate during repetitive stimulation at 100 Hz. The peak in the retardation signal did not summate, either, although the maintained component did (panel *B*; compare with Fig. 18 in Maylie et al., 1987*b*).

Repetitive stimulation was carried out on four fibers (Table V). A relatively high concentration of antipyrylazo III was used, usually 0.7–1.1 mM, so that the indicator-related absorbance change would be much larger than any movement-related artifact. As a result, the value of peak [Ca] associated with the first action potential (Table V, column 5) was smaller than that obtained earlier when the

fiber contained no more than 0.4 mM indicator (Table IV, column 6). The average value of peak [Ca] in Table V, column 5, was 1.75 μM.

In six runs, the Ca signal did not summate during 10 action potentials at 100 Hz, whereas in two other runs, marked by values greater than unity in column 7 of Table V, it did. In these two runs, the half-widths of the Ca signal produced by a single action potential (column 4) had the largest values in the table and were more than twice the mean value from freshly prepared, minimally perturbed

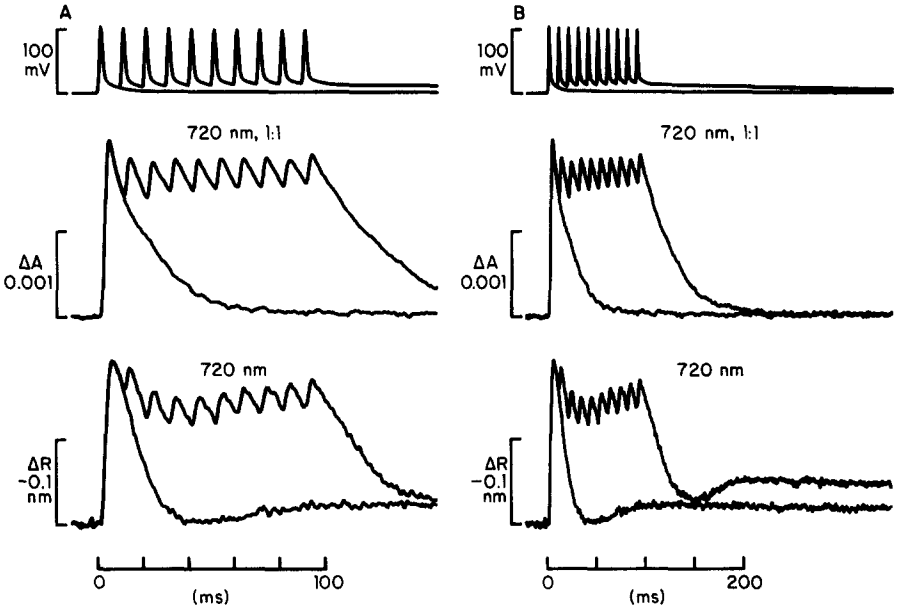

FIGURE 16. ΔA(720, 1:1) and ΔR(720) signals associated with 1 and 10 action potentials, mode 2 recording. Panels *A* and *B* show the same traces but displayed on different time scales. In each panel, the upper pair of superimposed traces shows the action potentials (the actual amplitude of the first one was 144 mV); the middle pair shows ΔA(720, 1:1) corrected for the intrinsic contribution using a 0.1-kHz Gaussian digital filter for the 810-nm trace and $n = 1.58$ and 1.24 for the 1 and 10 action potential traces, respectively; the bottom pair shows ΔR(720). The ΔR(720) and ΔR(810) signals were essentially the same; the ΔR(720) signal was selected for the figure because it had less noise. Fiber 092684.1; sarcomere spacing, 4.1 μm; Ringer's solution; temperature, 16.9°C; antipyrylazo III concentration, 0.80–0.82 mM; time after saponin treatment, 77–78 min.

fibers (Table IV, column 5). Thus, summation of the Ca signal may be linked to whatever changes underlie the broadening of the Ca signal. Since summation does not seem to be typical of Ca signals obtained from cut fibers early in an experiment, values from these two runs have not been included in the average values in columns 6 and 7.

Column 6 of Table V gives the value of [Ca] reached either at the end of the tetanus or during the plateau, depending on whether the Ca signal summated or

not. The average value from the six runs that did not show summation was 1.46 μM.

Column 7 of Table V gives the ratio of plateau [Ca] divided by peak [Ca] associated with the first action potential. We believe that the average value, 0.81, from the six runs that did not show summation is the best available estimate of this ratio measured in cut fibers containing antipyrylazo III and studied relatively early in an experiment.

TABLE V

Parameters Associated with Ca Signals Elicited by 1 and 10 Action Potentials

(1) Fiber reference	(2) Time after saponin treatment	(3) Indicator concentration	(4) Half-width	(5) First [Ca] peak	(6) Plateau [Ca]	(7) Plateau: first peak
	min	*mM*	*ms*	μM	μM	
062184.2	189	1.05	22.6	1.41	2.49*	1.77*
071184.2	63	0.45	10.9	2.05	1.49	0.73
	87	1.07	15.2	1.13	0.80	0.71
092684.1	78‡	0.81	15.3	1.49	1.21	0.81
	103	0.82	16.9	1.42	1.20	0.85
102185.1§	45	0.34	12.1	2.35	1.97	0.84
	61	0.73	16.8	2.28	2.08	0.91
	92	1.08	23.0	1.86	1.97*	1.06*
Mean				1.75	1.46	0.81
SEM				0.16	0.20	0.03

Column 1 gives fiber reference. Column 2 gives the time that elapsed between saponin treatment and the 10-action-potential measurement. Column 3 gives the internal concentration of antipyrylazo III. Column 4 gives the half-width of the $\Delta A(720, 1{:}2)$ or $\Delta A(720, 1{:}1)$ signal associated with a single action potential, taken 1–2 min before the 10-action-potential train. Column 5 gives free [Ca] at the first peak in the train. Column 6 gives, for all fibers except 062184.2, the average level of [Ca] between the 5th and 10th peak in the train; for fiber 062184.2, it gives the average level of [Ca] between the 9th and 10th peak; column 7 gives the ratio of column 6 to column 5. Free [Ca] was calculated from Eq. 1 using parameters given in the Methods; all the antipyrylazo III was assumed to be able to react normally with Ca. If only freely diffusible indicator can react (see Table VII), the average value in column 7 is reduced to 0.76 (SEM 0.04). The average temperature was 17.8°C.

* Values from runs that showed summation and were therefore not included in the averages (see text).

‡ Mode 2 recording (mode 1 was used in all other runs).

§ Values from an experiment performed by one of us (J.M.) a year after the other experiments were done; information from this fiber has not been included in the other tables.

Relative Timing of the Action Potential and Three Optical Signals

Mode 2 recording allows simultaneous measurement of the Ca, retardation, and intrinsic absorbance signals, making it possible to compare their time courses in a single sweep. Fig. 17 shows four superimposed traces, scaled to give the same peak magnitude, taken from a fiber that contained 0.3 mM antipyrylazo III. In order of times to half-peak, the waveforms show the action potential, the indicator-related $\Delta A(720, 1{:}1)$ or Ca signal, the retardation signal $[\Delta R(810)]$, and the intrinsic absorbance signal $[\Delta A(810, 1{:}1)]$.

In this example, there is a delay of 3.00 ms between the time to half-peak of the action potential and that of the Ca signal; an additional 0.52 ms separates the Ca signal and the retardation signal. The average values for these delays in fibers that contained ~0.3 mM indicator are 3.07 ms (data from 18 fibers, column 4 of Table IV) and 0.69 ms (data from 2 fibers, not shown), respectively. The average delay between times to half-peak of the action potential and

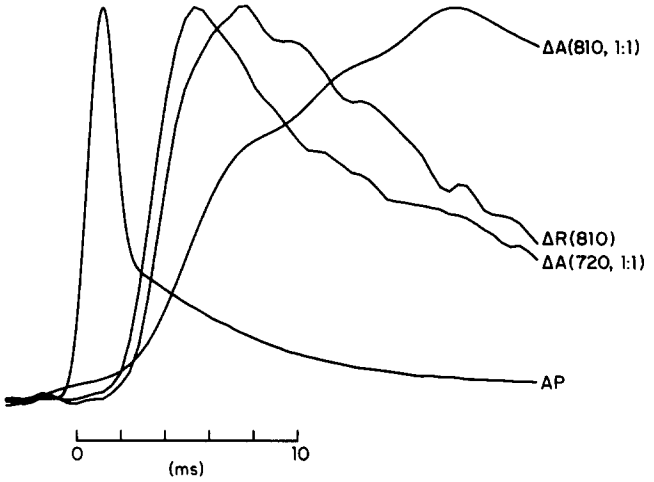

FIGURE 17. Relative time course of the action potential (AP), antipyrylazo III Ca signal [ΔA(720, 1:1)], retardation signal [ΔR(810)], and intrinsic absorbance signal [ΔA(810, 1:1)]. The four traces, obtained from a single set of mode 2 records, have been scaled to the same peak value and have been plotted on an expanded time scale; the negative-going ΔR(810) and ΔA(810, 1:1) signals have been plotted with inverted polarity. A cubic spline function (Greville, 1968) was used to draw the action potential from the digitized experimental points; the points in the other traces were connected by straight line segments. The action potential waveform was distorted by the 0.625-kHz eight-pole Bessel filter: the earliest electrical change preceded the $t = 0$ mark (determined by shifting zero time 1.6 ms to the right to correct for the low-frequency delay of the Bessel filter) and the peak was suppressed relative to the afterpotential. Nevertheless, the time to half-peak on the rising phase still provides a reliable indicator of timing (Fig. 16 in Irving et al., 1987). The ΔA(810, 1:1) record was filtered by a 0.1-kHz digital Gaussian filter. Same experiment as in Fig. 13; antipyrylazo III concentration, 0.298 mM; time after saponin treatment, 62 min; temperature, 17.9°C.

retardation signal, 3.76 ms, is in good agreement with the average value of 3.60 ms in fibers that did not contain indicator (column 9 of Table IV in Irving et al., 1987).

The intrinsic absorbance signal in Fig. 17 reached its half-maximum value after the retardation signal. This delay was a consistent finding.

Optical Signals Associated with Depolarization under Voltage Clamp

Effect of Antipyrylazo III Concentration and Experiment Duration on the Ca Signal Associated with Brief Depolarization

As expected, the progressive broadening of the Ca signal observed in action potential experiments was also observed with voltage-clamp depolarizations. Fig. 18 shows a voltage-clamp experiment in which a 5-ms depolarization to 0 mV was used to roughly mimic the depolarization of an action potential. Panel *A*

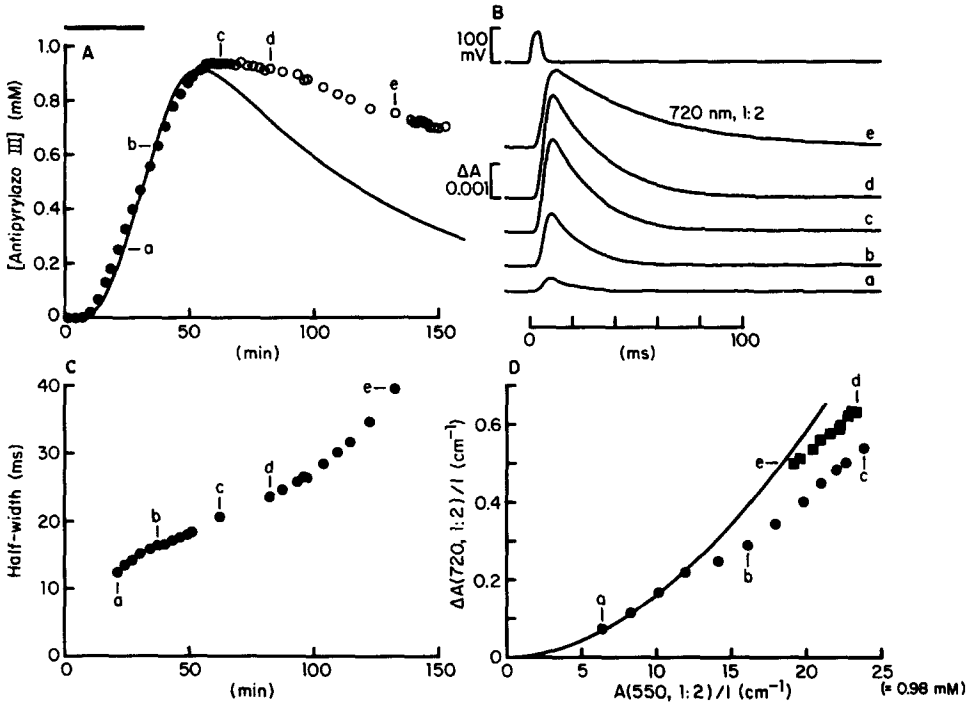

FIGURE 18. $\Delta A(720, 1{:}2)$ signals produced by 5-ms voltage-clamp pulses to 0 mV. Same format as Figs. 6–8. (*A*) Concentration of indicator plotted as a function of time after its addition to the end pools 20 min after saponin treatment. The theoretical curve was obtained by fitting the equations for diffusion plus linear reversible binding to the filled circles; the parameters are given in columns 4 and 5 of Table II. (*B*) Voltage and five $\Delta A(720, 1{:}2)$ traces. The 720-nm signals have been corrected for the intrinsic contribution; the 810-nm signals were filtered with a 0.05-kHz Gaussian digital filter and $n = 0.39$ (*a*), 1.03 (*b*), 2.04 (*c*), and 1.00 (*d* and *e*). (*C*) Half-width of the $\Delta A(720, 1{:}2)$ signal plotted against time. (*D*) Peak $\Delta A(720, 1{:}2)/l$ plotted against $A(550, 1{:}2)/l$ or indicator concentration, with ● and ■ denoting data taken during the period of increasing and decreasing, respectively, antipyrylazo III concentration. The continuous curve was calculated from Eq. 1 using [Ca] = 2.74 μM, obtained by fitting the ● data for antipyrylazo III concentrations $\leq$0.4 mM. Fiber 101684.1; sarcomere spacing, 3.9 μm.

shows the time course of the indicator concentration at the optical recording site; the theoretical curve was calculated from the equations for diffusion plus linear reversible binding. In panel *B*, the top trace shows voltage recorded during a 5-ms step to 0 mV. The next five traces show Ca signals recorded at different times. As with action potential stimulation, the amplitude of the Ca signal became larger as the indicator concentration increased and the duration of the signal became longer as the experiment progressed.

Fig. 18*D* shows the peak amplitude of the Ca signal plotted against indicator concentration. From *a* to *b* to *c*, the experimental points increase monotonically, with a slight dip to the left of point *b*. The jump between points *c* and *d* may have resulted from stimulation; eight voltage steps, each one lasting 100 ms and depolarizing the membrane to −50 to +20 mV, were imposed at 2–3 min intervals. Apart from the 5-ms pulses to 0 mV, the only other stimulation in this experiment was a series of 200-ms near-threshold pulses taken just before *c* and just after *e*.

Fig. 18*C* shows the half-width of the Ca signal plotted against time. The duration of the signal progressively increased during the time course of the experiment.

Ca signals elicited by brief voltage-clamp pulses were routinely monitored in five pulsed-exposure experiments. In all fibers, the signals changed with the indicator concentration and experiment duration in the manner shown in Fig. 18, *C* and *D* (except for the jump between *c* and *d*); in one case, however, the effect of experiment duration on half-width was small. These changes are similar to those found using action potential stimulation (Figs. 6–9).

Determination of the Intrinsic Contribution to Long-Duration Voltage-Clamp Signals

In some experiments, the method described in Fig. 5 for estimating the intrinsic contribution failed to work with long-duration voltage-clamp signals. Fig. 19 shows an example in which the method worked early in an experiment (*A*), but failed later (*B*). In *A*, the top trace shows the voltage recorded during a 200-ms pulse to −51 mV. The next set of three traces shows superimposed changes in 1:2 uncorrected absorbance at 550, 720, and 810 nm, the three wavelengths routinely used with antipyrylazo III. A linear combination of the 810- and 720-nm traces was least-squares fitted to the 550-nm trace. The 550-nm trace is replotted underneath with the fit superimposed. The two curves are in good agreement and the scaling constants give, for the λ^{-n} intrinsic correction, a value $n = 1.62$, which is well within the range determined from action potential experiments. The bottom trace shows the Ca signal obtained in the usual way using this value of n.

The set of traces in Fig. 19*A* was taken relatively early in the experiment, just before trace *c* in Fig. 18. Fig. 19*B* shows a second set taken later, after *e* in Fig. 18. The top trace shows the voltage recorded during a pulse to −60 mV. The next three traces show uncorrected 1:2 absorbance similar to the traces in *A*, except that the maintained levels of the 720- and 810-nm traces are positive

rather than negative. No linear combination of the 720- and 810-nm waveforms gave a good fit to the entire 550-nm trace, but it was possible to obtain a reasonable fit to the first part of the trace, as is shown. Both scaling constants were negative, which means that the intrinsic contribution to either the 720- or 550-nm trace must be negative, i.e., the polarity of the intrinsic signal at 720 or 550 nm must be opposite to that at 810 nm. These changes in intrinsic contribution from panel *A* to *B* were not accompanied by much change in the electrical

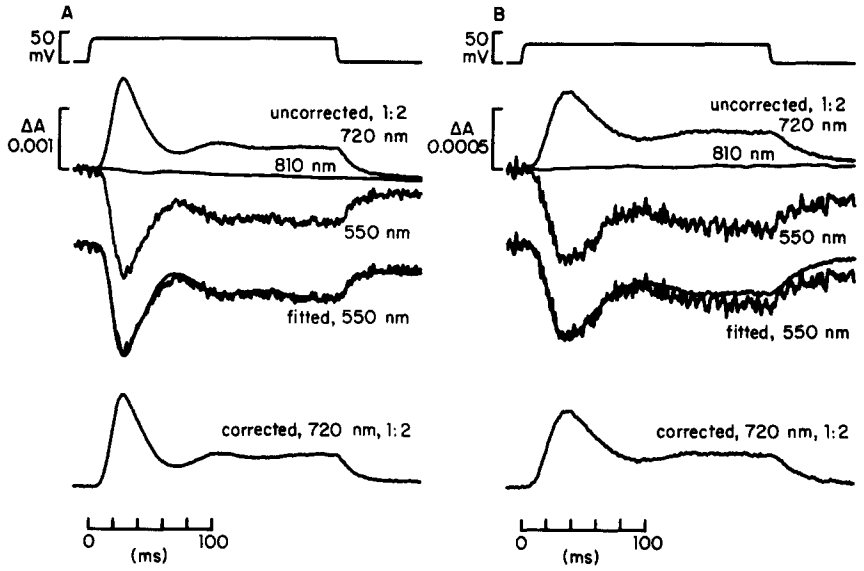

FIGURE 19. Optical traces produced by a small 200-ms depolarization using voltage clamp. (*A*) Traces taken early during an experiment. The top trace shows the voltage record associated with a pulse to −51 mV. The next traces show $\Delta A(\lambda, 1{:}2)$ superimposed for λ = 720, 810, and 550 nm without correction for the intrinsic contribution. The traces labeled "fitted, 550 nm" show the $\Delta A(550, 1{:}2)$ trace, repeated, and the best-fit linear combination of $\Delta A(720, 1{:}2)$ and $\Delta A(810, 1{:}2)$ based on scaling constants −1.176 and 3.294, respectively. These scaling constants give n = 1.62, and this value has been used to estimate the intrinsic contribution to the $\Delta A(720, 1{:}2)$ trace. The corrected trace is shown at the bottom. (*B*) Traces taken later in the experiment. Similar in layout to *A*, depolarization to −60 mV. The scaling constants for the best fit to the 550-nm trace were −1.22 for the 720-nm trace and −0.572 for the 810-nm trace, determined from the first two-sevenths of the traces (the entire time course was used in *A*). As described in the text, the negative sign of both scaling constants prevents the intrinsic correction from being estimated in the usual way; consequently, to obtain the bottom trace, n was arbitrarily set equal to 1. The set of records used in *A* was obtained 77 min after saponin treatment (indicator concentration, 0.93 mM), and the set in *B* was obtained 158 min after saponin treatment (indicator concentration, 0.73 mM). The 810-nm records were filtered digitally with a 0.05-kHz Gaussian filter. Same experiment as in Fig. 18.

condition of the fiber; the holding current increased from −22 to −28 nA, the resting membrane resistance decreased from 0.171 to 0.138 MΩ·cm, and the ratio $r_e/(r_e + r_i)$ decreased from 0.986 to 0.977.

Such a change in polarity with the wavelength of the intrinsic signal has not been directly observed without indicator and is rarely found indirectly, with indicator, except in voltage-clamp experiments using depolarizations lasting 0.1 s or longer. It may be related to movement or to the appearance of maintained signals, probably associated with a change in pH or free [Mg], which will be described in a later article. Since the 810-nm trace in Fig. 19*B* is small compared with the 720-nm trace, however, the intrinsic correction is relatively unimportant; consequently, n was arbitrarily set equal to 1, close to the average value 1.1 observed without indicator (Table III, column 6, in Irving et al., 1987). The indicator-related 720-nm signal is shown at the bottom of Fig. 19*B*. Although the intrinsic correction is somewhat uncertain, it is adequate for the analysis of the signals in the following section.

Ca Signals Recorded Near Threshold

Fig. 20*A* shows Ca signals associated with depolarizing pulses to various voltages near threshold. Two sets of records were taken at different times on the same fiber. The top trace shows an example of a voltage record; the middle traces show Ca signals from the first set of records, taken relatively early in the experiment, 74–82 min after saponin treatment (one run is illustrated in Fig. 19*A*); the lower traces show Ca signals from the second set of records, taken 158–169 min after saponin treatment (one run is illustrated in Fig. 19*B*).

A pronounced feature of the first set of Ca signals (middle traces) is the presence of an oscillatory or oscillation-like response. The absorbance change at −60 mV is small and difficult to evaluate. The traces at the other three voltages, however, show an early peak followed by a damped oscillation superimposed on a maintained level. Records taken at more depolarized potentials (not shown) did not show oscillatory behavior. The circles in Fig. 20*B* show the peak free [Ca], estimated from the middle set of traces in Fig. 20*A*, plotted semilogarithmically against membrane potential. The response was steeply voltage dependent; the line, fitted through the data obtained with the smallest depolarizations, corresponds to an e-fold change every 1.9 mV.

The second set of Ca signals (bottom traces in Fig. 20*A*) is less peaky and oscillatory than the first set. In addition, they have a different voltage dependence, as shown by the ×'s in Fig. 20*B*. The relation between the logarithm of peak [Ca] and voltage has been shifted to more negative potentials and the steepness has been reduced. The straight line corresponds to an e-fold change every 3.4 mV.

The shift of the peak [Ca] curve to more negative potentials and the decrease in steepness were consistently observed during the time course of cut muscle fiber experiments. They were found in two other experiments using antipyrylazo III. In one fiber, the e-fold factor was 2.1 mV 54–64 min after saponin treatment and was 2.6 mV 20–25 min later. In the other fiber, the factor was 2.3 mV 79–84 min after saponin treatment and was 5.6 mV ~70 min later. Similar changes were also found in two experiments using arsenazo III (Maylie et al., 1987*b*).

In Fig. 20*A*, the bottom traces also differ from the middle traces in that, after the voltage pulse, the Ca signal returned to baseline more slowly. This slowing also occurred with stronger depolarizations (not shown). Kovacs et al. (1983*a*) were the first to report such a decrease in the rate of decay of the Ca signal during the time course of an experiment. They attributed the effect to the

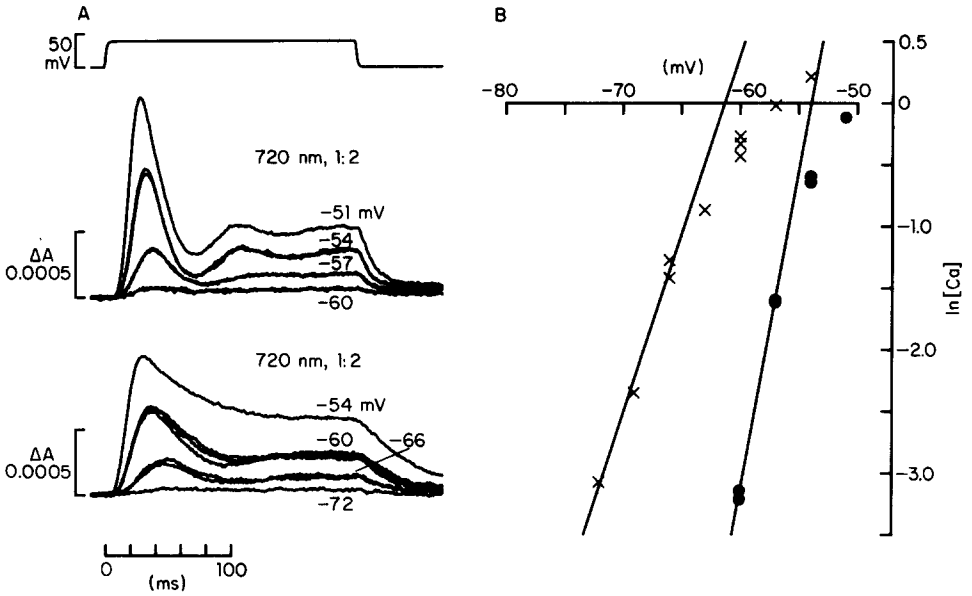

FIGURE 20. Effect of experiment duration on ΔA(720, 1:2) traces recorded with small depolarizations. Same experiment as in Figs. 18 and 19. (*A*) The top trace is a representative voltage record. The middle set of traces shows superimposed Ca signals recorded at the four voltages indicated with bracketing measurements included; this set was taken 74–82 min after saponin treatment, with 0.91–0.94 mM antipyrylazo III and a holding potential of −90 mV. The lower set shows superimposed traces taken 158–169 min after saponin treatment, with 0.73–0.70 mM indicator and the same holding potential. The middle traces have been corrected for the intrinsic signal using $n = 1.6$, the average value obtained by the procedure illustrated in Fig. 19*A*. The lower traces have been corrected using $n = 1$ as described in Fig. 19*B*. (*B*) Peak values of logarithm of [Ca] (in micromolar) plotted against voltage during the step. The calibration used Eq. 1 and assumed that all the indicator was available to react normally with Ca. (●) From the earlier run illustrated by the middle set of traces in *A*. The slope of the straight line indicates an e-fold change in peak [Ca] every 1.91 mV. (×) From the later run illustrated by the bottom set of traces in *A*. The straight line corresponds to an e-fold change in peak [Ca] every 3.41 mV.

increase in the concentration of antipyrylazo III that occurred during their experiments. This explanation does not apply to the results in Fig. 20*A*, however, since the indicator concentration decreased with time; it was 0.91–0.94 mM when the middle traces were taken and 0.73–0.70 mM when the bottom traces were taken. This slowing effect, consistently observed in our pulsed-exposure

voltage-clamp experiments, is probably due to the same factors that increase the half-width of the Ca signal in pulsed-exposure action potential experiments, i.e., a change in the physiological state of cut fibers during the experiment.

DISCUSSION

Myoplasmic Diffusion and Binding of Antipyrylazo III

With respect to myoplasmic diffusion and binding, the results with antipyrylazo III are similar to those obtained with arsenazo III (Maylie et al., 1987*b*): most of the indicator inside a fiber is bound to or sequestered by myoplasmic constituents (Table II*A*, column 5); the binding produces little change in the spectral characteristics of the indicator (Figs. 3 and 4); after pulsed exposure, the indicator usually leaves the central region of a fiber more slowly than it entered (Fig. 1*C*); and once binding has been taken into account, the value of the free diffusion constant for indicator entering a cut fiber is similar to that measured for molecules of similar size moving along skinned fibers (Table II*A*, column 6). The binding sites for antipyrylazo III have not been identified but are unlikely to be associated with the sarcoplasmic reticulum since the indicator does not bind to sarcoplasmic reticulum vesicles isolated from skeletal muscle (Scarpa, A., personal communication quoted in Kovacs et al., 1979).

Perhaps the most difficult result to explain is that, after pulsed exposure, antipyrylazo III, like arsenazo III (Maylie et al., 1987*b*), usually does not rapidly leave the optical site although it can still react, apparently almost normally, with Ca (Figs. 8*D* and 14*B*). This is not related to either exposure to light or electrical stimulation (p. 94). Four explanations for this phenomenon have been considered and none seems entirely satisfactory.

(*a*) Reversible binding with saturation. In this article, the time course of the antipyrylazo III concentration at the optical site has been analyzed using equations for diffusion plus linear reversible binding, i.e., the extent of binding at any particular time is assumed to be directly proportional to the concentration of free indicator (Fig. 1). Baylor et al. (1986) injected up to 3 mM antipyrylazo III into an intact fiber and measured the concentration at different times along the fiber. They fitted their results with equations derived from diffusion plus nonlinear reversible binding in which binding was characterized by equilibrium of a first-order reaction capable of saturation. No evidence for saturation was found in our experiments in which smaller concentrations of indicator were used (Fig. 1*B*). In addition, the type of reversible saturation used by Baylor et al. (1986) would not be expected to explain the failure of indicator to leave the recording site after pulsed exposure (Fig. 1*C*).

(*b*) Irreversible binding. Since antipyrylazo III usually fails to diffuse out of the central region of a fiber as rapidly as it diffuses in, the possibility of slow irreversible binding should be considered. A simple model, using both linear reversible and linear irreversible binding (Eqs. 10 and 11 in Maylie et al., 1987*b*), gave theoretical curves that usually matched the experimental time course of indicator concentration (Fig. 2). The values obtained for the diffusion constant of free indicator, D (Table III, column 4), however, were unreasonably large for

a molecule the size of antipyrylazo III (p. 94). Another difficulty is that in many experiments the relation between peak $\Delta A(720)$ and $A(550)$ was reversible (e.g., Fig. 8*D*) and large Ca signals were measured at late times, when most of the indicator was estimated to be irreversibly bound (Fig. 2*B*). This raises the question of whether irreversibly bound antipyrylazo III can react rapidly with Ca to form Ca:indicator complexes having a 1:2 stoichiometry.

(*c*) Diffusion barrier. This explanation supposes that a barrier to diffusion slowly develops during the time course of an experiment. One possibility is that after saponin treatment the end-pool segments of a fiber slowly revert to being impermeable to indicator. Another possibility is that some kind of internal barrier develops that hinders the movement of indicator from one sarcomere to the next. Although an explanation of this type may be correct, it must be consistent with two sets of observations: (*i*) the barrier retards the movement of indicator in experiments with antipyrylazo III (and possibly arsenazo III, Maylie et al., 1987*b*), but not with tetramethylmurexide (Maylie et al., 1987*a*), and (*ii*) in antipyrylazo III experiments, the barrier does not develop before antipyrylazo III is added to the end-pool solutions (Table II*B* and p. 94).

(*d*) Reversible binding, the characteristics of which change with time after exposure to antipyrylazo III. Generally, as mentioned in *b*, the reversibility of the relation between peak $\Delta A(720)$ and $A(550)$ suggests that the fraction of indicator available to react with Ca does not depend on time per se but may vary with the indicator concentration. Hence any change in indicator binding during the course of an experiment should not change the ability of indicator to react with Ca. Several schemes of this sort can be proposed and it is difficult with the available information to rule them out.

Although the explanation is uncertain, it is clear that most of the antipyrylazo III inside a muscle fiber is not freely dissolved in myoplasm. The processes associated with its binding or sequestration are complex and may have irreversible components. Such binding or sequestration raises important questions concerning the interpretation of antipyrylazo III Ca signals. Is bound or sequestered indicator able to react with Ca? If so, is it still able to form Ca:indicator complexes having a 1:2 stoichiometry? Is the affinity for Ca changed? Is the speed of reaction with Ca altered?

Properties of the Ca Signal Associated with Action Potential Stimulation in a Minimally Perturbed Fiber

Table IV gives timing parameters of Ca signals recorded in freshly prepared cut fibers that contained 0.3 mM antipyrylazo III. On average, the Ca signal, at 18°C, reached halfway to peak 3.07 ms later than the action potential (column 4) and had a half-width of 10.1 ms (column 5).

The value of 10 ms for the half-width is close to that found by Baylor et al. (1982*b*) in a single experiment, at 20°C, on an intact fiber containing 0.76 mM antipyrylazo III (given by 0.53 mM divided by 0.7 for the path length). The value is smaller, however, than those reported by others who made more extensive measurements. Palade and Vergara (1982) give an average value of 15.5 ms in six cut fibers studied at room temperature, probably 21–22°C (their

Table IV, indicator concentration not given but probably ≥1 mM), and Baylor et al. (1983*b*) give an average value of 20.9 ms for five intact fibers, at 16.5–17.4°C, containing 0.9–2.1 mM indicator (their Table I). These two sets of half-width measurements were made with a higher concentration of indicator than was used in the fibers in Table IV and this may account for some of the difference between their results and ours.

The value of 10 ms for the half-width is also close to that found in cut fibers, at the same temperature, containing small amounts of arsenazo III, 0.1 mM for example. With arsenazo III, the half-width depends steeply on the indicator concentration; at 0.5–1.0 mM, the values are more than twice those at 0.1 mM and are similar in both intact and cut fibers (Maylie et al., 1987*b*). This steep concentration dependence may explain the observation that, in intact fibers, the half-width of a Ca signal recorded with 0.5–1.1 mM arsenazo III is about twice that recorded with 0.6–1.5 mM antipyrylazo III (Baylor et al., 1983*b*).

In the experiments listed in Table IV, the average amount of Ca complexed by 0.3 mM antipyrylazo III was 7.4 μM. Since this amount is much smaller than that complexed by troponin (column 6 in Tables VI and VII), the Ca signal should be minimally perturbed by the Ca-buffering capacity of the indicator. Hence, in a minimally perturbed, freshly prepared cut fiber at 18°C, after action potential stimulation, the best estimate of the half-width of an antipyrylazo III Ca signal is 10 ms; it seems possible that the half-width of the Ca signal in a minimally perturbed intact fiber would be the same.

This value of 10 ms for half-width (Table IV, column 5) applies to the change in antipyrylazo III absorbance, $\Delta A(720)$. The half-width of the free [Ca] waveform is somewhat smaller, 8.0–9.4 ms (column 3 in Tables VI and VII), because the relation between Δ[Ca] and $\Delta A(720)$ is not strictly linear. If antipyrylazo III does not react with Ca instantaneously, but with a delay (Baylor et al., 1985; Maylie et al., 1987*a*), the estimate for the half-width of the free [Ca] transient would be further reduced and its estimated amplitude would be increased.

In calibrating the magnitude of free [Ca] (Eq. 1), the usual assumption is that all the indicator inside a fiber is able to react normally with Ca. On this assumption, peak free [Ca] is 3.11 μM after a single action potential in a minimally perturbed fiber (Table IV, column 6). But suppose that only those indicator molecules that are free to diffuse can react with Ca. The concentration of $[Ap]_T$ in Eq. 1 should then be multiplied by $1/(R + 1)$ (obtained from Table IIA, column 5). Analyzing the data used for Table IV in this way gives an average peak free [Ca] of 42 μM (6 μM SEM; results not shown). With 0.3 mM total antipyrylazo III and the average value for $(R + 1)$, 3.149, the average peak concentration of $[CaAp_2]$, 7.4 μM, corresponds to 16% of free indicator being complexed with Ca.

These two different assumptions for calibration, namely that bound indicator reacts either normally with Ca, giving peak free [Ca] = 3 μM, or not at all, giving [Ca] = 42 μM, represent extremes. It seems likely that the correct myoplasmic calibration lies somewhere in between. For example, a 1:2 Ca:antipyrylazo III complex might be made from two free indicator molecules or from one free and one bound molecule, but not from two molecules bound to spatially separated sites.

Equilibrium Binding of Ca by Troponin

Contraction in vertebrate twitch muscle is enabled by Ca ions binding to Ca-regulatory sites on troponin (Ebashi et al., 1969). In reconstituted thin filaments from rabbit muscle, these sites bind Ca according to a 1:1 binding isotherm with a dissociation constant of ~2 μM if myosin is not present (Potter and Zot, 1982, temperature not given; Rosenfeld and Taylor, 1985, 20°C), a situation that should resemble that found in a highly stretched muscle fiber, such as we used, with no overlap of thick and thin filaments.

The extent of Ca complexation during activity will depend on the amplitude of the free [Ca] transient and, if the transient is brief, on its duration and the speed with which Ca reacts with troponin. As discussed below, the Ca:troponin reaction is sufficiently fast that equilibrium binding should be approximately established during a brief tetanus. According to Table V, column 7, the plateau value of free [Ca] associated with a 100-ms tetanus at 100 Hz is ~0.8 times the peak value associated with a single action potential. If the low Ca calibration is used, peak free [Ca] = 3.1 μM in a minimally perturbed cut fiber (Table IV, column 6) and the plateau value should be 3.1 × 0.8 = 2.5 μM; with the dissociation constant of troponin given above, a fraction 0.56 of the Ca-regulatory sites on troponin should be occupied. If the high Ca calibration is used, peak free [Ca] = 42 μM (see above), plateau [Ca] should equal 34 μM, and 0.94 of the sites on troponin should be occupied.

In intact frog twitch fibers, moderately stretched and injected with aequorin, the level of tension produced by a brief tetanus appears to be near maximum since it is not further increased by maneuvers that produce a higher level of myoplasmic free [Ca] as assessed by aequorin luminescence (Blinks et al., 1978; Lopez et al., 1981). The interpretation of these studies, carried out at temperatures similar to those used here, was that a brief tetanus produced nearly maximum activation of contraction. In highly stretched fibers, with no overlap of thick and thin filaments, the extent of activation must be estimated in some way other than by measuring tension. One approach is to measure the change in intensity of the second actin layer line in the X-ray diffraction pattern, a change thought to be associated with a lateral movement of tropomyosin on the surface of the thin filaments that occurs soon after Ca binds to the Ca-regulatory sites on troponin (Huxley, 1972). Kress et al. (1986), using frog semitendinosus muscles, have found that the maximum intensity change during a brief tetanus is approximately the same in muscles stretched beyond filament overlap as in those maintained at rest length. Thus, a brief tetanus appears to produce nearly maximum activation in both moderately and highly stretched frog twitch fibers.

This raises the question of how much Ca needs to be bound to troponin to produce maximum activation. Fuchs and Fox (1982) measured tension and bound Ca in the same preparation of glycerinated rabbit psoas fibers at 22°C. Both measurements increased as free [Ca] was increased and reached a saturating level at [Ca] $\approx$ 10 μM. The relation between tension and bound Ca was linear in the range where the amount of bound Ca was 50–100% of maximum. In these experiments, maximum activation corresponded to complete saturation of the Ca-binding sites. Blanchard et al. (1984) compared Ca binding and Mg-ATPase activity in rabbit psoas myofibrils. They showed that the ATPase activity in-

creased monotonically with the amount of Ca bound and that maximum activity required complete saturation of the Ca-binding sites. These studies suggest that maximum activation of both contraction and Mg-ATPase activity in rabbit muscle requires that Ca be bound to all the available Ca-regulatory sites on troponin.

If the results of these studies on rabbit muscle can be applied to intact or cut frog fibers, the implication is clear: the level of myoplasmic free [Ca] produced during a brief tetanus should be able to complex nearly all the Ca-regulatory sites on troponin. The antipyrylazo III [Ca] transient fails to do this if the low Ca calibration is used. It succeeds, however, if the high Ca calibration is used. The following article (Maylie et al., 1987*a*) will show that results obtained with tetramethylmurexide are consistent with the idea that the free [Ca] transient is much greater than 3 μM.

Kinetic Analysis of Binding of Ca to Troponin and Parvalbumin after Action Potential Stimulation

If the [Ca] transient is brief, such as that after an action potential, Ca binding to troponin cannot be considered to be in equilibrium. In this case, the time course of Ca binding to troponin, and also to parvalbumin, can be calculated provided that the reaction sequence and rate constants for Ca binding are known. The aim of this section is to carry out such calculations; they can then be used to estimate net Ca movement from the sarcoplasmic reticulum into myoplasm.

Rosenfeld and Taylor (1985) studied the kinetics of Ca binding to the Ca-regulatory sites on troponin in reconstituted thin filaments from rabbit muscle. To explain the effect of Ca concentration on the measured association rate constant, they invoked the reaction sequence

$$\mathrm{Ca} + \mathrm{T} \underset{}{\overset{K_0}{\rightleftharpoons}} \mathrm{CaT} \underset{k_{-1}}{\overset{k_1}{\rightleftharpoons}} \mathrm{CaT_1}. \qquad \text{(I)}$$

According to this sequence, Ca reacts instantaneously with the Ca-free site T. This site has a relatively low affinity for Ca, characterized by an association constant $K_0 = 4 \times 10^4\ \mathrm{M}^{-1}$ (or a dissociation constant equal to 25 μM). CaT is then converted to $\mathrm{CaT_1}$, the more tightly binding form of the site, with forward and backward rate constants k_1 and k_{-1}. If $[\mathrm{Ca}] < K_0^{-1}$, the characteristics of reaction sequence I are similar to those of the sequence

$$\mathrm{Ca} + \mathrm{T} \underset{k_{-1}}{\overset{k_1 K_0}{\rightleftharpoons}} \mathrm{CaT_1}. \qquad \text{(II)}$$

If $[\mathrm{Ca}] \ll K_0^{-1}$, the two reaction sequences are kinetically indistinguishable.

Although equilibrium binding of Ca to reconstituted thin filaments obeys a simple 1:1 binding isotherm, kinetic studies indicate that the two Ca-regulatory sites on each troponin do not bind Ca in an identical and noninteracting fashion (Rosenfeld and Taylor, 1985). At 4°C, two values were obtained for k_1K_0, 0.7×10^7 and $2 \times 10^7\ \mathrm{M}^{-1}\ \mathrm{s}^{-1}$, and two values for k_{-1}, 15–20 and 1.5–2.0 s^{-1}; at 20°C, two values are given for k_{-1}, 140–200 and 15–20 s^{-1}, but none for k_1K_0.

To calculate Ca binding to troponin from our [Ca] transients, values of rate

constants appropriate for 18°C should be used. These could be estimated, by geometrical interpolation, from values at 4 and 20°C if k_1K_0 at 20°C were known. Since a direct measurement is not available, k_1K_0 must be estimated indirectly. One method of estimation is to use reaction sequence II and known values of k_{-1} and the equilibrium binding constant. A difficulty arises, though, with using data from reconstituted thin filaments because there are two values of k_{-1} and it is not clear how these should be incorporated into either reaction sequence I or II. The situation is simpler with Ca binding to complexes of either troponin:tropomyosin or reconstituted thin filaments plus myosin subfragment 1; in either case, the two Ca-regulatory sites on troponin appear to be identical and noninteracting and only one value of k_{-1} is obtained. Using this method of estimation, values of k_1K_0 at 20°C are three to five times the corresponding values at 4°C and are equal to 0.5×10^8 M^{-1} s^{-1} for troponin:tropomyosin and $0.6–0.8 \times 10^8$ M^{-1} s^{-1} for reconstituted thin filaments plus subfragment 1. Since, at 4°C, the two values of k_1K_0 for reconstituted thin filaments (0.7×10^7 M^{-1} s^{-1} and 2×10^7 M^{-1} s^{-1}) lie close to the range of k_1K_0 for troponin:tropomyosin (1×10^7 M^{-1} s^{-1}) and reconstituted thin filaments plus subfragment 1 (2×10^7 M^{-1} s^{-1}), it seems reasonable to assume that they also do so at 20°C. Thus, k_1K_0 for reconstituted thin filaments is likely to be $0.5–0.8 \times 10^8$ M^{-1} s^{-1} at 20°C and $0.4–0.7 \times 10^8$ M^{-1} s^{-1} at 18°C.

In previous calculations, Baylor et al. (1983*a*) used reaction sequence II to describe Ca binding to troponin. For their model 2, the forward rate constant was taken as 0.575×10^8 M^{-1} s^{-1} at 15–17°C, based on the measurements of Johnson et al. (1981), at 25°C, and an assumed factor of 2 to compensate for the difference in temperature. Since this value is consistent with the estimate derived above, $0.4–0.7 \times 10^8$ M^{-1} s^{-1}, it will be used here. We will also use the backward rate constant from model 2 (Baylor et al., 1983*a*), 115 s^{-1}, which, using reaction sequence II, gives a dissociation constant of 2 μM, consistent with equilibrium binding measurements of Ca to reconstituted thin filaments from rabbit muscle (Potter and Zot, 1982; Rosenfeld and Taylor, 1985).

The following calculations of Ca binding to troponin use reaction sequence II rather than I. With the low Ca calibration, $[Ca] \ll K_0^{-1}$, so that the calculations of Ca binding to troponin should be reasonably accurate. With the high Ca calibration, however, peak $[Ca] \approx K_0^{-1}$. In this case, the calculations may be rather approximate when free [Ca] is near peak value. Another oversimplification in the calculations is that the two Ca-regulatory sites on thin filaments are considered to be identical and noninteracting, a situation, as mentioned above, that is inconsistent with the results from kinetic measurements (Rosenfeld and Taylor, 1985).

The computational procedure uses the free [Ca] transient obtained from the experimentally measured absorbance change (Ca signal) to calculate the time course and extent of Ca binding to the major myoplasmic buffer systems. These buffers include the Ca-regulatory sites on troponin (denoted by [CaTrop], myoplasmic concentration of sites taken as 0.24 mM), the Ca,Mg sites on parvalbumin ([CaParv], myoplasmic concentration 1 mM), and the indicator itself ($[CaAp_2]$). Total myoplasmic Ca, denoted by $[Ca]_T$, is given by $[Ca]_T = [Ca] +$

$[CaAp_2]$ + [CaTrop] + [CaParv]; the net Ca flux from the sarcoplasmic reticulum, release minus uptake, is given by the time derivative $d[Ca]_T/dt$. The rate constants used for the computations, taken from model 2 in Baylor et al. (1983*a*), are given in the legend to Fig. 21. The only change made in the parameters was that resting [Mg] was set at 1 mM, whereas in the previous article it was 2 mM.

Single action potential stimulation. The Ca signal used for the first set of calculations was taken from Fig. 5. This signal, obtained with 0.3 mM indicator, is typical of one from a minimally perturbed fiber in that the parameters given in columns 4–6 of Table IV (fiber 060884.2) are similar to the corresponding average values. Free [Ca] was computed from the absorbance change in two ways, using the extreme-case assumptions described above. In the first case, all the indicator was assumed to be able to react normally with Ca; this gave a value of 3.06 μM for peak free [Ca] (Table VI, column 4). In the second case, only freely diffusible indicator was assumed to react with Ca; this gave a value of 23.6 μM (Table VII, column 4). Such large values of peak free [Ca] have also been estimated from tetramethylmurexide Ca signals (Maylie et al., 1987*a*), so that conclusions based on the high-estimate antipyrylazo III Ca signals apply equally well to tetramethylmurexide signals.

Fig. 21 shows paired results from the two sets of calculations, one using the low estimate of free [Ca] and the other using the high estimate. Within each pair, the trace with the larger amplitude was obtained with the high Ca estimate. The bottom trace shows the time course of $[CaAp_2]$ obtained by scaling the ΔA(720, 1:2) signal in Fig. 5*B*. The pair of traces above this shows free [Ca] estimated from Eq. 1 using the two extreme-case assumptions described above.

Each [Ca] waveform in Fig. 21 was then used to calculate the time course of Ca binding to troponin. The results are shown in the pair of traces plotted above the [Ca] traces. They show that, at peak occupancy, 109 μM of Ca-regulatory sites are complexed with Ca if the small [Ca] transient is used, whereas 216 μM are complexed if the large transient is used. These values correspond to fractional site occupancies of 0.45 and 0.90, respectively.

The next two pairs of traces show [MgParv] and [CaParv]. At the time that Ca binding to troponin is maximal, parvalbumin has complexed, above the resting level, 57 μM Ca in the case of the small [Ca] transient and 66 μM Ca in the case of the large transient. At late times, when Ca binding to troponin has returned nearly to baseline level, parvalbumin has complexed 77 μM Ca (small transient) and 105 μM Ca (large transient). Thus, with the small [Ca] transient, troponin releases ~109 μM Ca during relaxation and parvalbumin takes up $77 - 57 = 20$ μM Ca; with the large [Ca] transient, troponin releases 216 μM Ca and parvalbumin takes up $105 - 66 = 39$ μM. These numbers indicate that, with either amplitude [Ca] transient, for each five Ca that leave troponin after peak occupancy, approximately one is bound (transiently) by parvalbumin and four are (presumably) taken up by the sarcoplasmic reticulum. Thus, according to the model, parvalbumin serves to transiently buffer ~20% of the Ca that dissociates from troponin during mechanical relaxation at 18°C.

The next pair of traces in Fig. 21 shows the time course of total myoplasmic Ca, $[Ca]_T$. The peak value gives a minimum estimate of the amount of Ca

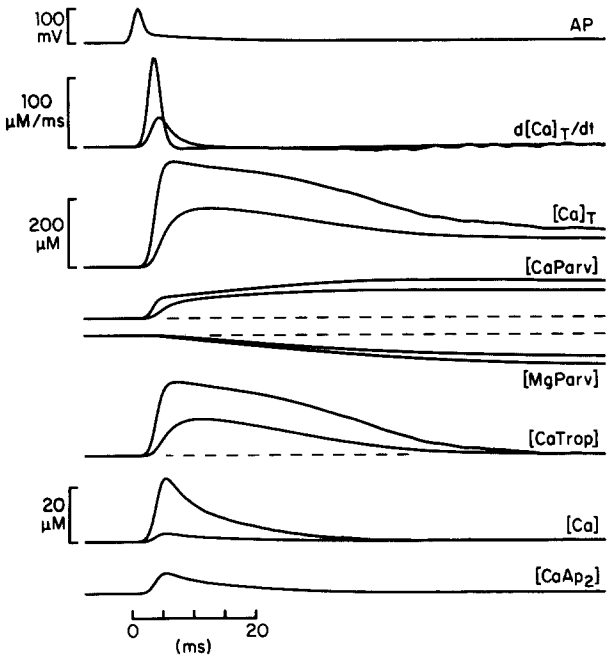

FIGURE 21. Modeling of Ca movements in myoplasm after a single action potential. The calculations are based on model 2 of Baylor et al. (1983*a*), except that free [Mg] was set at 1 instead of 2 mM; the myoplasmic concentration of Ca-regulatory sites on troponin was taken as 240 μM, the K_D as 2 μM, the forward rate constant as 0.575×10^8 M^{-1} s^{-1}, and the backward rate constant as 115 s^{-1}; the concentration of Ca,Mg sites on parvalbumin was taken as 1 mM, the K_D for Ca as 4 nM (with the forward rate constant equal to 1.25×10^8 M^{-1} s^{-1} and the backward rate constant equal to 0.5 s^{-1}), and the K_D for Mg as 91 μM (with the forward rate constant equal to 3.3×10^4 M^{-1} s^{-1} and the backward rate constant equal to 3.0 s^{-1}). The uppermost trace shows the action potential (AP) and the lowermost trace, labeled "[$CaAp_2$]," shows the concentration of the Ca:antipyrylazo III complex. This was calculated, after slight modification, from the ΔA(720, 1:2) signal in Fig. 5*B*. First, the prestimulus baseline was set constant to its average value; this level corresponds to the assumed value of 0.02 μM for resting free [Ca]. Second, the final portion of the curve, after 0.3 times peak value, was smoothed by a 51-point quadratic routine (Hamming, 1977). Third, a slightly different wavelength dependence was used for the intrinsic correction, $n = 1.00$ instead of 1.63, so that the signal would decay to baseline level by the end of the plotted trace. The pair of traces above [$CaAp_2$] shows free [Ca]. The trace with the smaller amplitude was calculated on the assumption that all the indicator was able to react normally with Ca; peak free [Ca] = 3.06 μM. The trace with the larger amplitude was calculated assuming that only freely diffusible indicator, estimated as $1/(R + 1)$ times total indicator with $(R + 1) = 2.555$, was able to react with Ca; peak free [Ca] = 23.6 μM. The four next pairs of traces, from bottom to top, represent: [CaTrop], the concentration of Ca bound to Ca-regulatory sites on troponin; [MgParv], the concentration of Mg bound to Ca,Mg sites on parvalbumin; [CaParv], the concentration of Ca bound to Ca,Mg sites on parvalbumin; and $[Ca]_T$, the concentration of total myoplasmic Ca, calculated from $[Ca]_T$ = [Ca] + [$CaAp_2$] + [CaTrop] + [CaParv]. The baseline values are [CaTrop] = 2.4 μM, [MgParv] = 647.1 μM, [CaParv] = 294.1 μM, and $[Ca]_T$ = 296.6 μM. The 200-μM vertical calibration bar applies to all four pairs of traces. The uppermost pair of traces shows $d[Ca]_T/dt$. In each of the six pairs, the trace with the smaller amplitude is associated with the smaller [Ca] transient.

released from the sarcoplasmic reticulum. This amount was 175 μM in the case of the small [Ca] transient and 313 μM in the case of the large transient.

The top pair of traces in Fig. 21 shows $d[Ca]_T/dt$, which, as mentioned above, gives the net Ca flux from the sarcoplasmic reticulum into myoplasm. The peak rates of net movement into myoplasm were 41 μM/ms for the small [Ca] transient and 116 μM/ms for the large transient. After the early positive peak, there was a smaller negative phase, barely discernible at the vertical scale used in the figure, corresponding to net movement out of myoplasm, which, according to the model, would be mediated by the sarcoplasmic reticulum Ca pump. The peak rates for this negative phase were -2.7 μM/ms for the small transient and -2.9 μM/ms for the large transient.

Tables VI and VII give results of similar calculations carried out for the 18 fibers used in Table IV. The average values in column 6 correspond to a fraction 0.46 of the Ca-regulatory sites on troponin becoming complexed with Ca if the low Ca calibration is used and 0.93 becoming complexed if the high Ca calibration is used. These values are slightly smaller than the corresponding values obtained above for the fractional occupancy during a brief tetanus, 0.56 and 0.94, respectively.

In Fig. 21, the curves calculated from the 3.06 μM [Ca] transient are similar in many ways to curves calculated from transients obtained from intact fibers injected with either arsenazo III (Baylor et al., 1983*a*) or antipyrylazo III (Quinta-Ferreira et al., 1984*b*). The average values of parameters computed for cut fibers containing antipyrylazo III, using the low Ca calibration, are given in Table VI of this article; corresponding values for intact fibers injected with arsenazo III are given in Table IV of Baylor et al. (1983*a*). The main differences between the two sets of results are that we find with antipyrylazo III (*a*) a reduced peak fractional occupancy of troponin Ca-regulatory sites (0.46 compared with 0.60), (*b*) a larger peak sarcoplasmic reticulum Ca flux associated with the Ca pump (2.5 μM/ms compared with 1.5 μM/ms), and (*c*) a reduced contribution of parvalbumin to relaxation (complexing one out of five Ca coming off troponin rather than two out of three Ca). These differences are due primarily to the relatively brief, more rapidly decaying free [Ca] transient estimated with 0.3 mM antipyrylazo III, which had an average half-width of 9.4 ms at 18°C (Table VI, column 3), compared with that estimated by Baylor et al. (1983*a*) with 0.18–0.84 mM arsenazo III, which had an average half-width of 35.9 ms at 15–17°C. This difference in half-width is probably due to the slow component of the arsenazo III Ca signal (Baylor et al., 1983*b*; Quinta-Ferreira et al., 1984*a*).

The brief duration of the antipyrylazo III Ca transient results in a large minimum value of $d[Ca]_T/dt$, with an average magnitude of 2.51 μM/ms for the low Ca calibration (Table VI, column 11) and 4.18 μM/ms for the high Ca calibration (Table VII, column 11). According to the model, this represents a lower limit on the peak rate of operation of the sarcoplasmic reticulum Ca pump. Since the myoplasmic concentration of pump-associated Ca-binding sites is probably 0.2–0.5 mM (Table I in Baylor et al., 1983*a*), the turnover rate per pump molecule inside a fiber should be 5–13 s^{-1} for the low Ca calibration and 8–21 s^{-1} for the high Ca calibration. Two biochemical studies provide direct estimates

of this turnover rate in isolated sarcoplasmic reticulum vesicles. In vesicles from rabbit muscle, the turnover rate is 10–12 s^{-1} at 25°C (with millimolar amounts of ATP, Verjovski-Almeida and Inesi, 1979) and in vesicles from bullfrog muscle it is 7 s^{-1} at 15°C (based on data from Ogawa et al., 1981; see p. 659 in Baylor et al., 1983*a*). Our model-derived values are somewhat larger than these measured values but not seriously so. Our values would be reduced if parvalbumin

TABLE VI

Computed Ca Movements Associated with a Single Action Potential, Using the Low Ca Calibration

(1)	(2)	(3)	(4)	(5)	(6)	(7)	(8)	(9)	(10)	(11)
	Free [Ca]			[CaTrop]		$[Ca]_T$	$d[Ca]_T/dt$			
Fiber reference	Time to half-peak	Half-width	Peak	Time to half-peak	Peak	Peak	Time to half-peak	Half-width	Peak	Minimum
	ms	*ms*	*μM*	*ms*	*μM*	*μM*	*ms*	*ms*	*μM/ms*	*μM/ms*
060884.1	2.97	7.93	2.71	4.59	97.2	157.8	2.50	3.55	38.5	−2.74
060884.2	3.30	9.22	3.06	4.87	109.0	175.0	2.79	3.56	41.4	−2.69
061184.1	3.15	8.60	4.92	4.54	139.8	213.3	2.55	3.14	60.8	−3.36
061184.2	3.18	7.03	3.85	4.61	118.7	184.2	2.63	3.23	51.3	−4.05
061284.2	3.30	8.20	3.77	4.81	121.2	188.4	2.73	3.43	49.3	−3.21
061384.1	2.93	8.26	3.09	4.55	106.4	170.3	2.44	3.44	43.9	−3.32
061484.2	3.09	10.71	3.14	4.78	111.5	178.4	2.59	3.54	44.2	−1.95
061484.3	3.06	11.13	3.31	4.59	115.4	184.5	2.51	3.61	44.5	−2.09
061984.2	4.03	10.18	3.07	5.77	109.6	174.2	3.45	3.85	41.6	−1.82
062184.2	3.04	9.30	3.01	4.64	106.1	171.8	2.54	3.47	41.8	−2.39
062284.1	2.81	7.92	3.38	4.32	112.5	178.6	2.33	3.29	46.6	−2.97
062284.2	3.22	8.04	3.85	4.69	122.3	189.2	2.63	3.41	50.1	−2.70
062584.1	3.89	11.34	3.11	5.63	112.8	180.7	3.28	3.83	41.4	−2.17
070584.1	2.98	9.38	2.87	4.64	104.1	168.3	2.51	3.55	40.4	−1.77
071184.2	2.68	9.37	2.18	4.39	87.4	147.7	2.21	3.91	31.3	−2.46
092484.1	2.97	11.58	2.28	4.86	91.0	153.3	2.54	3.79	34.2	−1.40
092684.1	2.49	11.51	2.50	4.46	99.0	161.4	2.05	3.72	39.8	−1.72
111684.1	3.18	9.14	2.86	4.82	103.2	167.2	2.67	3.55	40.7	−2.32
Mean	3.13	9.38	3.16	4.75	109.3	174.7	2.61	3.55	43.4	−2.51
SEM	0.09	0.33	0.15	0.09	2.9	3.6	0.08	0.05	1.6	0.16

Ca signals were measured early in the experiment in minimally perturbed fibers containing 0.3 mM antipyrylazo III. Column 1 gives fiber reference. Column 2 gives the interval between the time to half-peak of the action potential and the time to half-peak of free [Ca]. Column 3 gives the half-width of the free [Ca] transient. Column 4 gives peak free [Ca]. Free [Ca] was calculated from indicator-related $\Delta A(720)$ (see Methods) on the assumption that all the antipyrylazo III was able to react normally with Ca. Columns 5 and 6 give the time to half-peak (after time to half-peak of the action potential) and peak value, respectively, of [CaTrop], calculated as described in the text. Column 7 gives the peak value of $[Ca]_T$. Columns 8–11 give information about the flux of Ca across the sarcoplasmic reticulum membrane: column 8 gives time to half-peak (after time to half-peak of the action potential); column 9 gives half-width; column 10 gives the maximum value of net flux; column 11 gives the minimum value of net flux, with the negative sign representing uptake into the sarcoplasmic reticulum. Although the same $\Delta A(720)$ signals used in Table IV were used here, the corresponding values in columns 2 and 3 here and columns 4 and 5 there are somewhat different; this is because free [Ca] is not a strictly linear function of $\Delta A(720)$, so that the free [Ca] waveform is slightly different from the absorbance waveform. Average temperature, 17.9°C.

either were present in greater concentration or reacted with Ca more rapidly than assumed, or if Ca dissociated from troponin less rapidly than assumed (for example, if the calculations had used the slower of the two dissociation rate constants observed in reconstituted thin filaments by Rosenfeld and Taylor, 1985). It is also possible that the uptake of Ca by the sarcoplasmic reticulum has a rapid early phase or that the turnover rate of pump molecules in intact sarcoplasmic reticulum membranes inside a fiber is greater than that in isolated vesicles.

TABLE VII

Computed Ca Movements Associated with a Single Action Potential, Using the High Ca Calibration

(1)	(2)	(3)	(4)	(5)	(6)	(7)	(8)	(9)	(10)	(11)
	Free [Ca]			[CaTrop]		$[Ca]_T$	$d[Ca]_T/dt$			
Fiber reference	Time to half-peak	Half-width	Peak	Time to half-peak	Peak	Peak	Time to half-peak	Half-width	Peak	Minimum
	ms	*ms*	*μM*	*ms*	*μM*	*μM*	*ms*	*ms*	*μM/ms*	*μM/ms*
060884.1	3.07	6.99	31.0	3.10	221.1	320.5	1.98	2.00	145.4	−3.09
060884.2	3.39	8.19	23.6	3.51	216.3	312.6	2.32	2.26	115.9	−2.91
061184.1	3.38	6.45	107.0	2.81	231.6	415.1	1.84	1.76	238.9	−4.32
061184.2	3.32	5.96	50.9	3.09	228.8	349.4	1.96	1.95	184.8	−5.21
061284.2	3.49	6.47	81.0	2.96	234.7	384.1	2.00	1.83	202.7	−11.36
061384.1	3.06	6.97	45.3	2.96	229.7	344.2	1.89	1.83	186.3	−3.72
061484.2	3.27	8.13	79.2	2.86	229.3	363.3	1.77	1.80	233.3	−9.50
061484.3	3.22	8.69	62.5	2.72	230.5	363.5	1.78	1.88	190.4	−4.75
061984.2	4.13	9.07	24.0	4.38	214.4	295.3	2.92	2.32	141.6	−2.56
062184.2	3.16	7.79	39.7	3.01	225.1	334.6	2.00	1.93	152.5	−4.03
062284.1	2.90	6.98	28.4	3.02	220.3	322.4	1.98	1.91	144.4	−3.05
062284.2	3.36	6.82	43.2	3.15	231.2	342.5	1.95	2.11	164.8	−5.94
062584.1	4.01	9.75	32.4	4.00	221.5	321.2	2.62	2.27	147.7	−2.77
070584.1	3.07	8.18	28.7	3.17	220.4	320.8	2.03	2.03	141.3	−2.50
071184.2	2.79	8.13	33.9	2.55	230.7	344.0	1.52	2.23	119.2	−2.43
092484.1	3.06	10.00	25.7	3.32	213.2	299.2	2.10	1.99	149.0	−1.69
092684.1	2.55	10.38	20.1	3.14	212.5	285.1	1.67	2.01	181.6	−1.87
111684.1	3.22	8.55	11.5	3.96	190.5	270.2	2.41	2.54	96.1	−3.50
Mean	3.25	7.97	42.7	3.21	222.3	332.7	2.04	2.04	163.1	−4.18
SEM	0.09	0.30	5.9	0.11	2.5	8.4	0.08	0.05	9.1	0.60

Same format as Table VI except that only freely diffusible antipyrylazo III (estimated to equal total indicator concentration times $1/[R + 1]$, obtained from Table IIA, column 5) was assumed to be able to react with Ca.

Multiple action potential stimulation. Just after the repetitive stimulation records in Fig. 16 were obtained, the apparatus was switched from mode 2 to mode 1 recording to improve the signal-to-noise ratio, and the stimulation sequence was repeated (Fig. 22). Panels *A* and *B* show curves calculated using the low and high Ca calibrations, respectively. After a single action potential, peak free [Ca] was 1.43 μM in *A* and 12.4 μM in *B* (indicator concentration, 0.82 mM). These values are smaller than those determined earlier with 0.3 mM indicator (2.5 μM in Table VI [fiber 092684.1] and 20.1 μM in Table VII),

probably because of the difference in the indicator concentration (cf. Figs. 7*D* and 8*D*). Consequently, the absolute amounts of Ca bound to buffers in the single action potential calculations in Fig. 22 are smaller than the corresponding values in Fig. 21.

The approximately constant level of free [Ca] that develops during repetitive stimulation (Fig. 22) leads to an almost constant amount of Ca bound to troponin. The average value of [Ca] between the 5th and 10th peaks was 1.2 μM in *A* and

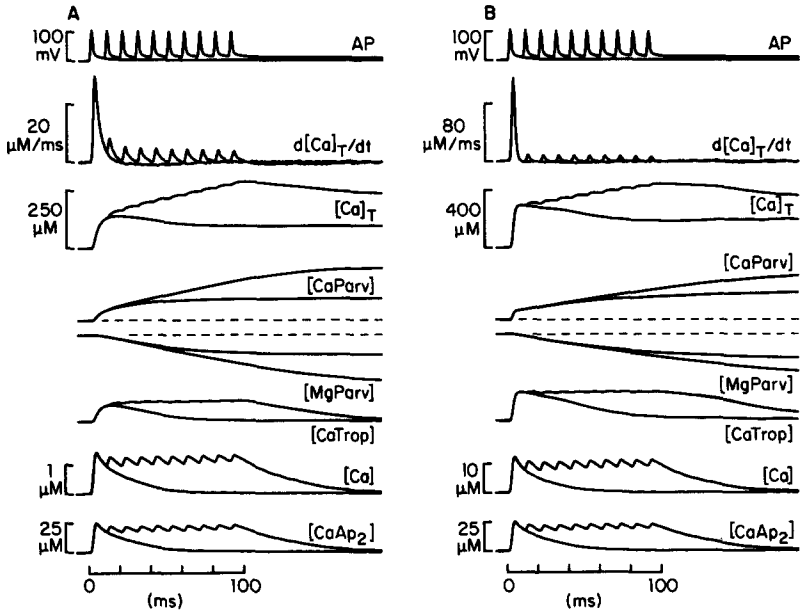

FIGURE 22. Modeling of Ca movements in myoplasm after either 1 or 10 action potentials. Same theoretical procedure and format as used in Fig. 21. (*A*) Superimposed traces associated with 1- or 10-action-potential stimulation. The calibration of the free [Ca] trace assumed that all the antipyrylazo III was available to react normally with Ca; this gave peak [Ca] = 1.43 μM after a single action potential. (*B*) Same as *A*, except that only freely diffusible antipyrylazo III, estimated as $1/(R + 1)$ times total indicator with $(R + 1) = 2.632$, was assumed to be able to react with Ca; peak [Ca] after a single action potential was estimated as 12.4 μM. Different vertical scales are used in *A* and *B*. Fiber 092684.1; intrinsic correction based on $n = 1$; sarcomere length, 4.1 μm; antipyrylazo III concentration, 0.82–0.81 mM; time after saponin treatment, 100–103 min; temperature, 17.0°C.

10 μM in *B*; the peak fractional occupancy of troponin was 0.38 in *A* and 0.83 in *B*, which is identical to that expected from steady state binding with $K_D = 2$ μM. The small amounts of net Ca released after the first one to two action potentials, shown most clearly in the $d[Ca]_T/dt$ traces, do not bind to the contractile filaments. They represent the amounts taken up by parvalbumin in response to the maintained level of [Ca].

Fig. 23 shows the peak values of [CaTrop] (squares) and $[Ca]_T$ (circles), plotted

as a function of the number of action potentials. The data were taken from the curves in Fig. 22 and similar curves calculated from other runs made during the same experiment. Panels *A* and *B* show results using the low and high Ca calibrations, respectively.

In Fig. 23*A*, the average peak value of [CaTrop] after one action potential was 71 μM. This corresponds to a fractional occupancy of 0.30, which, as mentioned above, increased to 0.38 after 10 action potentials. The peak value of $[Ca]_T$ after 1 action potential, 140 μM on average, approximately doubled after 10 action potentials; this represents a minimum estimate of sarcoplasmic reticulum Ca release.

The values of [CaTrop] and $[Ca]_T$ in *B* are larger than those in *A*, as expected for the larger [Ca] transient. A single action potential gave peak [CaTrop] = 196 μM (0.82 fractional occupancy) and 10 action potentials gave 200 μM (0.83

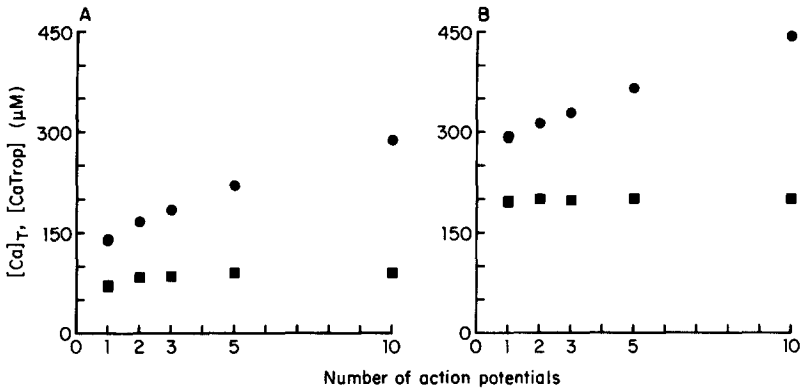

FIGURE 23. Effect of number of action potentials, 100 Hz stimulation, on the theoretical peak magnitudes of [CaTrop] (■) and $[Ca]_T$ (●), from the calculations in Fig. 22 and others based on records taken during the same experiment. Panel *A* shows results from the low Ca calibration and panel *B* shows results from the high calibration. In each panel, there are four bracketing measurements taken with 1 action potential and two bracketing measurements taken with 10 action potentials. Antipyrylazo III concentration, 0.84–0.79 mM; temperature, 17.0°C.

fractional occupancy). The peak value of $[Ca]_T$ was 293 μM after 1 action potential and was 1.5 times greater after 10 action potentials. Most of the increase in release, compared with *A*, is accounted for by the increase in Ca bound to the regulatory sites on troponin.

With both the low and high Ca calibrations, the fractional occupancy of Ca-regulatory sites on troponin is only slightly greater after 10 action potentials than after 1. This is consistent with the observation that, in frog muscle, the change in the intensity of the second actin layer line of the X-ray diffraction pattern, and presumably thin filament activation, is almost as great after a single action potential as during a brief tetanus (Kress et al., 1986).

Relative timing of the action potential and three Ca-related signals. The computational approach described above makes it possible to compare the time courses of free [Ca], [CaTrop], and $d[Ca]_T/dt$. Fig. 24 superimposes the action

potential and these three Ca-related signals from Fig. 21. The traces have been scaled to the same peak value and plotted on an expanded time base. Panels *A* and *B* refer to the low and high Ca calibrations, respectively, which, as mentioned above, should provide a bracket for the actual myoplasmic Ca calibration. The values of timing parameters from this and other experiments are given in Tables VI (low Ca calibration) and VII (high Ca calibration).

The average time to half-peak of $d[Ca]_T/dt$, after that of the surface action potential, was 2.61 ms using the low Ca calibration (Table VI, column 8) and 2.04 ms using the high Ca calibration (Table VII, column 8). These times should be corrected for any temporal delay between the action potential at the optical recording site and that at the Vaseline seal next to the left-hand voltage-recording

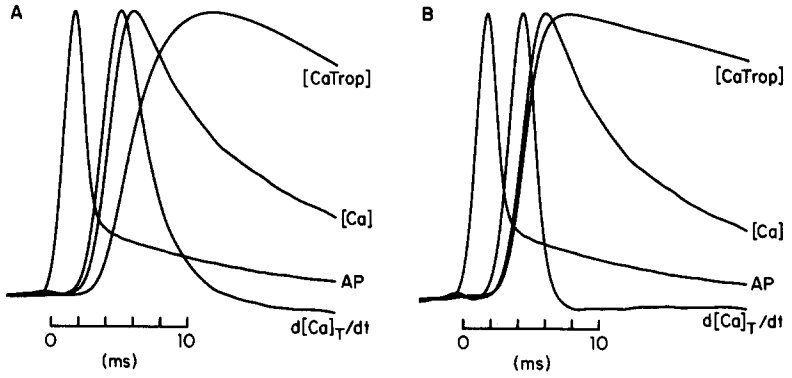

FIGURE 24. Comparison of waveforms of early events in excitation-contraction coupling. Panels *A* and *B* each show four waveforms that have been scaled to the same peak amplitude. The earliest waveform shows the action potential (AP); this has been distorted by the 0.625-kHz Bessel filter, as mentioned in the legend to Fig. 17. The second waveform shows $d[Ca]_T/dt$, which is assumed to represent Ca flux across the sarcoplasmic reticulum membrane. The third waveform shows free [Ca] and the fourth waveform shows [CaTrop]. The traces are taken from Fig. 21, with panel *A* showing the ones based on peak [Ca] = 3.06 μM and panel *B* showing the ones based on [Ca] = 23.6 μM. A cubic spline function (Greville, 1968) was used to interpolate between the experimental or calculated points in each trace.

end pool (Fig. 1 in Irving et al., 1987). Ideally, the electrical stimulus from the right-hand pool should depolarize the fiber in the central region uniformly to threshold, thereby making this delay zero. The fiber's cable properties prevent such uniform depolarization so that the action potential should develop first near the current-passing end pool and then move from right to left. The time to move from the optical recording site to the left-hand Vaseline seal should be short and no more than 0.1 ms, the delay for an action potential traveling at a velocity of 2 m/s (Hodgkin and Nakajima, 1972).

Thus, the total delay between the surface action potential at the optical site and Ca flux from the sarcoplasmic reticulum is in the range 2.1–2.7 ms. This delay includes the time required for the action potential to propagate into the

transverse tubular system and activate the Ca release mechanism. Since the propagation delay should be 0.5–1 ms for a 100-μm-diameter fiber at 18°C (Gonzalez-Serratos, 1971; Nakajima and Gilai, 1980), the activation delay in our experiments is probably no greater than 2 ms.

The half-width of $d[Ca]_T/dt$ was 3.55 ms using the low Ca calibration (Table VI, column 9) and 2.04 ms using the high Ca calibration (Table VII, column 9). This brief half-width of Ca flux imposes a kinetic constraint on the kinds of processes that might couple depolarization of the transverse tubules to sarcoplasmic reticulum Ca release. As one example, if chemical transmission were involved (Vergara and Tsien, 1985; Volpe et al., 1985), the half-width would be determined by the duration of the increase in transmitter concentration plus any delays introduced by the reaction of transmitter with receptor and subsequent steps leading to Ca release. In general, the half-time of removal or inactivation of transmitter must be less than the half-width of Ca release. A value in the range 2.04–3.55 ms for the half-width of Ca release implies, therefore, that the rate of removal or inactivation of transmitter is at least 200–300 s^{-1}. For prolonged activation, e.g., during a tetanus, such a rapid rate of removal would require, on the simplest scheme, that many transmitter molecules be produced at each tubular activation site. Since, under certain conditions, nearly maximum activation of contraction can be maintained for as long as 1 min (Gomolla et al., 1983), the amount of available transmitter or its precursor would need to be large or the stores would need to be replenished rapidly, within seconds.

Soon after the $d[Ca]_T/dt$ waveform begins (Fig. 24), free [Ca] and then [CaTrop] increase. [CaTrop] reaches its half-peak 4.75 ms after the action potential when the low Ca calibration is used (average value in Table VI, column 5) and 3.21 ms after the action potential when the high Ca calibration is used (Table VII, column 5). The time course of [CaTrop] can be compared with that of the increase in the intensity of the second actin layer line in the X-ray diffraction pattern (Kress et al., 1986). This increase, seen even in muscles stretched to largely eliminate overlap of thick and thin filaments, precedes the change in the intensity of the equatorial [1, 1] reflection produced by movement of cross-bridges toward the thin filaments. It is the earliest change observed in the X-ray diffraction pattern after stimulation and is attributed to movement of tropomyosin on the surface of the thin filaments. At 6°C, the X-ray change develops at about the same time in rest-length and highly stretched muscles (Kress et al., 1986). If the same similarity holds at 18°C, the X-ray change in a highly stretched fiber at this temperature should reach halfway to peak in 6.5 ms after stimulation (based on linear interpolation between values from rest-length muscles, 8.5 ms at 14°C and 4.5 ms at 22°C), which, allowing for the latency of action potential excitation, should correspond to a delay of ~6 ms after the time to half-peak of the surface action potential.

Several factors could contribute to the 1–3-ms delay between the calculated increase in [CaTrop] and the measured change in second actin layer line intensity: the estimate of Ca binding to troponin, based on reaction sequence II and identical, noninteracting sites, may be somewhat inaccurate; the change in X-ray intensity may be related in a nonlinear manner to the increase in [CaTrop] (for

example, the X-ray change may occur only after both Ca-regulatory sites are complexed); or there may be a delay between Ca binding to troponin and the change in X-ray intensity. The point we wish to emphasize is that the computed time course of [CaTrop] is sufficiently rapid to be consistent with the earliest change in the X-ray diffraction pattern. Consequently, the rate constants measured by Johnson et al. (1981) and Rosenfeld and Taylor (1985) for Ca binding to the Ca-regulatory sites on isolated rabbit troponin or troponin complexes may apply to troponin inside intact frog muscle fibers.

Since highly stretched muscle fibers, with no overlap of thick and thin filaments at the site of optical recording, were used in our experiments, the calculations of Ca binding to troponin were based on rate constants estimated from measurements on isolated troponin or troponin complexes in the absence of myosin. The affinity of reconstituted thin filaments for Ca is known to increase when myosin (Bremel and Weber, 1972) or myosin subfragment 1 (Rosenfeld and Taylor, 1985) is bound, however, so it is natural to wonder whether these calculations apply to an unstretched fiber that is able to contract. Kress et al. (1986) showed that, at 5–6°C, the intensity change of the equatorial [1, 1] reflection is only ~0.1 of maximum at the time when the intensity change of the second actin layer line is halfway to peak. Until this time, it would be surprising if myosin had much influence on Ca binding to troponin. If the same temporal relationship between the two intensity changes exists at 18°C, myosin should not influence Ca binding for the first 6 ms after the time to half-peak of the action potential. During this period, [CaTrop] increases to ~0.7 of peak value if the low Ca calibration is used (Fig. 24*A*) and almost reaches the peak if the high Ca calibration is used (Fig. 24*B*). Thus, after a single action potential in a fiber with overlapping thick and thin filaments, myosin should exert little influence on the binding of the first 70% of Ca to troponin and, in the case of the high Ca calibration, of the remaining Ca.

Once contraction is under way, however, myosin exerts an influence that would be expected to be maintained well into mechanical relaxation. After the [Ca] transient is over, Ca slowly dissociates from the Ca-regulatory sites on troponin and the intensity of the second actin layer line returns to baseline level. At 18°C, in fibers with overlapping filaments, the X-ray signal decays to half-peak at 53 ms after stimulation (based on linear interpolation between 75 ms at 14°C and 30 ms at 22°C, Kress et al., 1986). Similar measurements were not carried out at the same temperatures on highly stretched fibers, but at 6°C the rate of decay was found to be two to three times faster in highly stretched fibers than in ones held at rest length (Kress et al., 1986). This is consistent with myosin increasing the Ca affinity of reconstituted thin filaments (Bremel and Weber, 1972) by decreasing the rate of dissociation of Ca from the Ca-regulatory sites on troponin (Rosenfeld and Taylor, 1985). Thus, our calculated time course of Ca dissociating from troponin, which is appropriate for highly stretched fibers without overlap of thick and thin filaments (model 2 rate constants from Baylor et al., 1983*a*), might be faster than the actual time course of Ca dissociation in fibers having short sarcomere spacing.

In the present work, the time course of free [Ca] has been determined on the

assumption that the reaction between Ca and antipyrylazo III (Eq. 1) and the subsequent change in absorbance are sufficiently rapid that equilibrium holds at all times. Baylor et al. (1985) have provided indirect evidence that the change in antipyrylazo III absorbance tracks myoplasmic free [Ca] with a first-order delay of 1.4 ms, a finding consistent with our tetramethylmurexide results (Maylie et al., 1987*a*). The presence of such a delay would make the free [Ca] transient somewhat larger and briefer than estimated in Fig. 24 and elsewhere in this article, and would consequently decrease the calculated time to half-peak of [CaTrop].

Mechanisms Underlying the Early Retardation Signal

Suarez-Kurtz and Parker (1977) observed that, after action potential stimulation, the onset of the early retardation signal coincides with that of the arsenazo III Ca signal. They suggested that the change in retardation might be caused by the increase in myoplasmic free [Ca]. Since then, the time courses of the retardation and Ca signals after action potential stimulation have been compared using arsenazo III (in intact fibers, Baylor et al., 1982*b*, 1984; in cut fibers, Maylie et al., 1987*b*), antipyrylazo III (in intact fibers, Baylor et al., 1982*b*; in cut fibers, Figs. 13 and 17), and azo1 (in intact fibers, Hollingworth and Baylor, 1986). The time courses have also been compared using the voltage-clamp technique on cut fibers containing antipyrylazo III (Kovacs et al., 1983*b*). The similarity of onset found by Suarez-Kurtz and Parker has been consistently observed with all three indicators, although the time courses of the retardation and Ca signals are not identical.

The observation that the half-width of the retardation signal increases with time in the same manner as the half-width of the Ca signal supports the hypothesis that the retardation change is caused by the increase in myoplasmic Ca. Fig. 15*B* shows an experiment in which both half-widths increased, but by different amounts.

In the present work, two cut fibers, each containing 0.3 mM antipyrylazo III, had retardation signals with times to half-peak that lagged that of the Ca signal. The average delay was 0.69 ms. If the retardation signal is indeed a consequence of the increase in myoplasmic free [Ca], Ca complexation with antipyrylazo III must precede, by a fraction of a millisecond, the reaction between Ca and the myoplasmic receptor and subsequent events leading to the change in retardation.

The absence of a constant relation between the amplitudes of the retardation and Ca signals during an experiment was somewhat surprising. In Fig. 15*A*, the magnitude of the retardation signal increased from *b* to *d*, whereas peak free [Ca], estimated with antipyrylazo III, decreased. To explain this on the myoplasmic Ca hypothesis would require that the relation between retardation and free [Ca] change during the course of an experiment, at least in cut fibers, if the antipyrylazo III calibration is constant. Such a change could accompany a change in the oriented internal structure that produces the retardation signal. For example, either the rate constants associated with Ca binding or the structure's orientation might be altered. These interesting possibilities deserve future investigation.

Changes in Characteristics of Ca Signals during the Time Course of an Experiment

Most of the experiments described in this article lasted ≥2 h (Table I). During this time, four changes in the properties of Ca signals were consistently observed: the signal's half-width after action potential stimulation was increased (Figs. 6*C*, 7*C*, 8*C*, 9*A*, and 15*B*) or its return to baseline after a depolarizing voltage pulse was slowed (Figs. 18*C* and 20*A*); the voltage threshold was shifted to more negative potentials (Fig. 20*B*); the voltage dependence became less steep (Fig. 20*B*); and the oscillations recorded during threshold voltage steps became less marked (Fig. 20*A*).

The first three of these changes have also been observed with arsenazo III (Maylie et al., 1987*b*). The fourth change was difficult to evaluate with arsenazo III because the oscillatory responses, while present (Fig. 19*A* in Maylie et al., 1987*b*), were less marked. The reason for this is not known, but it may be due to the slow component of the arsenazo III Ca signal (estimated time constant, 10 ms, Quinta-Ferreira et al., 1984*a*) attenuating the oscillatory response.

The first change, the progressive broadening of the Ca signal, is produced primarily by a decrease in the rate of decay of the signal. This decrease was usually monitored by measuring the half-width of the Ca signal after action potential stimulation. Since the increase in half-width develops continually in pulsed-exposure experiments, even when the indicator concentration is decreasing, it cannot be explained solely by the Ca-buffering capacity of antipyrylazo III, although such buffering may influence the signal. Since in the same experiments the relation between peak $\Delta A(720)$ and indicator concentration was usually reversible, it seems unlikely that the early phase of Ca release from the sarcoplasmic reticulum is altered. Rather, sarcoplasmic reticulum Ca release might develop a late phase or the processes that remove free Ca from myoplasmic solution might become slowed.

Kovacs et al. (1983*a*) were the first to observe such a decrease in the rate of decay of the Ca signal during the time course of cut fiber experiments. In their experiments, carried out using voltage clamp, antipyrylazo III was continuously present in the end-pool solutions and its concentration inside the fiber always increased with time. They (and also Melzer et al., 1986) analyzed their results in terms of rapidly equilibrating Ca-binding sites intrinsic to the fiber; the progressive slowing of the Ca signal was assumed to be due exclusively to the increase in Ca buffering associated with the increase in indicator concentration. The results in this article show that this assumption is not correct, at least under our experimental conditions.

A clue concerning the cause of the increase in half-width is provided by the experiment shown in Fig. 6*C*. The increase in half-width developed more slowly in a notched fiber than in a fiber treated with saponin. This difference in time course could be explained quantitatively by assuming that the increase in half-width was produced by a change in the concentration of some substance(s) in the optical recording region and that this change developed more slowly in the notched fiber because the effective diffusion distance to the end pools was greater. The effect of path length on diffusion time, however, does not distin-

guish between substances that diffuse into the fiber from the end-pool solutions and those that are normally present in myoplasm and diffuse out after saponin treatment or notching.

Of the substances present in the end-pool solution, antipyrylazo III is unlikely to be responsible for the effect since the processes that underly the increase in half-width can develop in the absence of antipyrylazo III (Fig. 10, dashed lines). Thus, although antipyrylazo III may make a contribution to the increase in half-width, as possibly suggested by the comparison shown in Fig. 7*C*, the presence of indicator alone cannot explain all the effect. The concentration of glutamate is higher in the end-pool solution than in normal myoplasm, so it is possible that the increase in Ca signal duration is related to glutamate diffusion into the fiber. It is also possible that other differences between end-pool solution and myoplasm—for example, pH, free [Mg], or free [Ca]—might contribute to the time-dependent change. None of these possibilities can be ruled out.

It seems more likely, though, that the diffusible substances in question are normal constituents of myoplasm that progressively diffuse out of cut fibers. There are many possibilities: intrinsic Ca buffers, such as parvalbumin, that participate in relaxation; substances that regulate or modify the activity of the sarcoplasmic reticulum Ca pump or Ca release; or ions that move during Ca pump activity to provide electroneutrality, to name a few.

The modeling calculations described above bear on the possible role that parvalbumin might play. They indicate that parvalbumin complexes approximately one-fifth of the Ca released by troponin during relaxation. This fraction seems too small for a loss of parvalbumin to account for the two- to threefold increase in half-width observed in most experiments (Fig. 9). Parvalbumin might play a significant role, however, if its concentration or its speed of reaction with Ca were greater than assumed in the model.

One advantage offered by the cut fiber technique is the possibility of altering the composition of myoplasm to modify physiological function. The four changes in characteristics of the Ca signal mentioned at the beginning of this section may all be examples of such modification. These changes occur continually during an experiment on cut fibers, at least under our conditions, and can become rather prominent after several hours. Similar changes may occur in other experimental preparations derived from intact fibers, for example, in skinned fibers immersed in relatively large volumes of aqueous solution or in isolated sarcoplasmic reticulum vesicles. Such changes could occur rapidly after the removal of the sarcolemma, owing to the short diffusion distances involved, and could therefore go unnoticed. More needs to be done to understand these changes but we hope such understanding will provide useful information about the regulation of free [Ca] during muscle activation.

We thank the staff of the Yale Department of Physiology Electronics Laboratory for help with the design and construction of equipment. We also thank Drs. S. M. Baylor and L. B. Cohen for helpful discussion and for providing useful comments on the manuscript.

This work was supported by the U.S. Public Health Service grants NS-07474 and AM-37643. M.I. was initially a Science and Engineering Research Council Postdoctoral Fellow and subsequently a Royal Society University Research Fellow.

Original version received 5 May 1986 and accepted version received 15 September 1986.

REFERENCES

Baylor, S. M., W. K. Chandler, and M. W. Marshall. 1982*a*. Optical measurements of intracellular pH and magnesium in frog skeletal muscle fibres. *Journal of Physiology.* 331:105–137.

Baylor, S. M., W. K. Chandler, and M. W. Marshall. 1982*b*. Use of metallochromic dyes to measure changes in myoplasmic calcium during activity in frog skeletal muscle fibres. *Journal of Physiology.* 331:139–177.

Baylor, S. M., W. K. Chandler, and M. W. Marshall. 1982*c*. Dichroic components of Arsenazo III and Dichlorophosphonazo III signals in skeletal muscle fibres. *Journal of Physiology.* 331:179–210.

Baylor, S. M., W. K. Chandler, and M. W. Marshall. 1983*a*. Sarcoplasmic reticulum calcium release in frog skeletal muscle fibres estimated from Arsenazo III calcium transients. *Journal of Physiology.* 344:625–666.

Baylor, S. M., M. E. Quinta-Ferreira, and C. S. Hui. 1983*b*. Comparison of isotropic calcium signals from intact frog muscle fibers injected with Arsenazo III or Antipyrylazo III. *Biophysical Journal.* 44:107–112.

Baylor, S. M., S. Hollingworth, C. S. Hui, and M. E. Quinta-Ferreira. 1985. Calcium transients from intact frog skeletal muscle fibres simultaneously injected with Antipyrylazo III and Azo1. *Journal of Physiology.* 365:70P. (Abstr.)

Baylor, S. M., S. Hollingworth, C. S. Hui, and M. E. Quinta-Ferreira. 1986. Properties of the metallochromic dyes Arsenazo III, Antipyrylazo III and Azo1 in frog skeletal muscle fibres at rest. *Journal of Physiology.* 377:89–141.

Blanchard, E. M., B.-S. Pan, and R. J. Solaro. 1984. The effect of acidic pH on the ATPase activity and troponin Ca binding of rabbit skeletal myofilaments. *Journal of Biological Chemistry.* 259:3181–3186.

Blinks, J. R., R. Rudel, and S. R. Taylor. 1978. Calcium transients in isolated amphibian muscle fibres: detection with aequorin. *Journal of Physiology.* 277:291–323.

Bremel, R. D., and A. Weber. 1972. Cooperation within actin filament in vertebrate skeletal muscle. *Nature New Biology.* 238:97–101.

Colquhoun, D., and F. J. Sigworth. 1983. Fitting and statistical analysis of single-channel records. *In* Single-Channel Recording. B. Sakmann and E. Neher, editors. Plenum Press, New York. 191–263.

Ebashi, S., M. Endo, and I. Ohtsuki. 1969. Control of muscle contraction. *Quarterly Reviews of Biophysics.* 2:351–384.

Fuchs, F., and C. Fox. 1982. Parallel measurements of bound calcium and force in glycerinated rabbit psoas muscle fibres. *Biochimica et Biophysica Acta.* 679:110–115.

Gomolla, M., G. Gottschalk, and H. C. Luttgau. 1983. Perchlorate-induced alterations in electrical and mechanical parameters of frog skeletal muscle fibres. *Journal of Physiology.* 343:197–214.

Gonzalez-Serratos, H. 1971. Inward spread of activation in vertebrate muscle fibres. *Journal of Physiology.* 212:777–799.

Greville, T. N. E. 1968. Spline functions, interpolation, and numerical quadrature. *In* Mathematical Methods for Digital Computers. A. Ralston and H. S. Wilf, editors. John Wiley & Sons, Inc., New York. 156–168.

Hamming, R. W. 1977. Digital Filters. Prentice-Hall, Inc., Englewood Cliffs, NJ. p. 33.

Hodgkin, A. L., and S. Nakajima. 1972. Analysis of the membrane capacity in frog muscle. *Journal of Physiology.* 221:121–136.

Hollingworth, S., R. W. Aldrich, and S. M. Baylor. 1986. In vitro calibration of the metallochromic indicator dye Antipyrylazo III (ApIII). *Biophysical Journal.* 49:457*a*. (Abstr.)

Hollingworth, S., and S. M. Baylor. 1986. Calcium transients in frog skeletal muscle fibers injected with Azo1, a tetracarboxylate Ca indicator. *In* Optical Methods in Cell Physiology. P. De Weer and B. M. Salzberg, editors. John Wiley & Sons, Inc., New York. 261–283.

Huxley, H. E. 1972. Structural changes in the actin- and myosin-containing filaments during contraction. *Cold Spring Harbor Symposia on Quantitative Biology.* 37:361–376.

Irving, M., W. K. Chandler, J. Maylie, and N. L. Sizto. 1985. Antipyrylazo III calcium transients in cut frog twitch fibers. *Biophysical Journal.* 47:350*a*. (Abstr.)

Irving, M., J. Maylie, N. L. Sizto, and W. K. Chandler. 1987. Passive electrical and intrinsic optical properties of cut frog twitch fibers. *Journal of General Physiology.* 89:1–40.

Johnson, J. D., D. E. Robinson, S. P. Robertson, A. Schwartz, and J. D. Potter. 1981. Ca exchange with troponin and the regulation of muscle contraction. *In* Regulation of Muscle Contraction: Excitation-Contraction Coupling. A. D. Grinnell and M. A. B. Brazier, editors. Academic Press, Inc., New York. 241–259.

Kovacs, L., E. Rios, and M. F. Schneider. 1979. Calcium transients and intramembrane charge movement in skeletal muscle fibres. *Nature.* 279:391–396.

Kovacs, L., E. Rios, and M. F. Schneider. 1983*a*. Measurement and modification of free calcium transients in frog skeletal muscle fibres by a metallochromic indicator dye. *Journal of Physiology.* 343:161–196.

Kovacs, L., R. A. Schumperli, and G. Szucs. 1983*b*. Comparison of birefringence signals and calcium transients in voltage-clamped cut skeletal muscle fibres of the frog. *Journal of Physiology.* 341:579–593.

Kress, M., H. E. Huxley, A. R. Faruqi, and J. Hendrix. 1986. Structural changes during activation of frog muscle studied by time-resolved X-ray diffraction. *Journal of Molecular Biology.* 188:325–342.

Kushmerick, M. J., and R. J. Podolsky. 1969. Ionic mobility in muscle cells. *Science.* 166:1297–1298.

Lopez, J. R., L. A. Wanck, and S. R. Taylor. 1981. Skeletal muscle: length-dependent effects of potentiating agents. *Science.* 214:79–82.

Maylie, J., M. Irving, N. L. Sizto, G. Boyarsky, and W. K. Chandler. 1987*a*. Calcium signals recorded from cut frog twitch fibers containing tetramethylmurexide. *Journal of General Physiology.* 89:145–176.

Maylie, J., M. Irving, N. L. Sizto, and W. K. Chandler. 1987*b*. Comparison of arsenazo III optical signals in intact and cut frog twitch fibers. *Journal of General Physiology.* 89:41–81.

Melzer, W., E. Rios, and M. F. Schneider. 1986. The removal of myoplasmic free calcium following calcium release in frog skeletal muscle. *Journal of Physiology.* 372:261–292.

Nakajima, S., and A. Gilai. 1980. Radial propagation of muscle action potential along the tubular system examined by potential-sensitive dyes. *Journal of General Physiology.* 76:751–762.

Ogawa, Y., N. Kurebayashi, A. Irimajiri, and T. Hanai. 1981. Transient kinetics for Ca uptake by fragmented sarcoplasmic reticulum from bullfrog skeletal muscle with reference to the rate of relaxation of living muscle. *Advances in Physiological Science.* 5:417–435.

Palade, P., and J. Vergara. 1981. Detection of Ca with optical methods. *In* The Regulation of Muscle Contraction: Excitation-Contraction Coupling. A. D. Grinnell and M. A. B. Brazier, editors. Academic Press, Inc., New York. 143–158.

Palade, P., and J. Vergara. 1982. Arsenazo III and antipyrylazo III calcium transients in single skeletal muscle fibers. *Journal of General Physiology.* 79:679–707.

Potter, J. D., and H. G. Zot. 1982. The role of actin in modulating Ca binding to troponin. *Biophysical Journal.* 37:43*a*. (Abstr.)

Quinta-Ferreira, E., S. M. Baylor, and C. S. Hui. 1983. Comparison of Antipyrylazo III (Ap) and Arsenazo III (Az) signals from intact frog single muscle fibers. *Biophysical Journal.* 41:379*a*. (Abstr.)

Quinta-Ferreira, M. E., S. M. Baylor, and C. S. Hui. 1984*a*. Antipyrylazo III (Ap III) and Arsenazo III (Az III) calcium transients from frog skeletal muscle fibers simultaneously injected with both dyes. *Biophysical Journal.* 45:47*a*. (Abstr.)

Quinta-Ferreira, M. E., S. M. Baylor, and C. S. Hui. 1984*b*. Myoplasmic Ca transients and sarcoplasmic reticulum Ca movements in frog skeletal muscle fibres injected with Antipyrylazo III. *In* Book of Abstracts, 8th International Biophysics Congress, editor. IUPAB, Bristol. 207.

Rios, E., and M. F. Schneider. 1981. Stoichiometry of the reactions of calcium with the metallochromic indicator dyes Antipyrylazo III and Arsenazo III. *Biophysical Journal.* 36:607–621.

Rosenfeld, S. S., and E. W. Taylor. 1985. Kinetic studies of calcium binding to regulatory complexes from skeletal muscle. *Journal of Biological Chemistry.* 260:252–261.

Scarpa, A., F. J. Brinley, and G. Dubyak. 1978. Antipyrylazo III, a "middle range" Ca metallochromic indicator. *Biochemistry.* 17:1378–1386.

Suarez-Kurtz, G., and I. Parker. 1977. Birefringence signals and calcium transients in skeletal muscle. *Nature.* 270:746–748.

Vergara, J., and R. Y. Tsien. 1985. Inositol trisphosphate induced contractures in frog skeletal muscle fibers. *Biophysical Journal.* 47:351*a*. (Abstr.)

Verjovski-Almeida, S., and G. Inesi. 1979. Fast-kinetic evidence for an activating effect of ATP on the Ca transport of sarcoplasmic reticulum ATPase. *Journal of Biological Chemistry.* 254:18–21.

Volpe, P., G. Salviati, F. D. Virgilio, and T. Pozzan. 1985. Inositol 1,4,5-trisphosphate induces calcium release from sarcoplasmic reticulum of skeletal muscle. *Nature.* 316:347–349.